Identifying the Surfaces of Human Protein TPP1 and Telomerase RNA that Interact with One Another to Improve Enzyme Function and Association at the Telomere

By Caitlin Bell

Molecular, Cellular, and Developmental Biology Thesis Defense
April 5th, 2012

Cech Laboratory
University of Colorado – Boulder
Department of Chemistry and Biochemistry
Boulder, CO. 80309-0215

Primary Thesis Advisor: Dr. Thomas Cech, Ph.D.

Defense Committee Members: Dr. Rui Yi, Ph.D., Dr. James Goodrich, Ph.D., and Dr. Thomas Cech, Ph.D.

Abstract

Telomerase is a cellular reverse transcriptase that adds tracts of telomeric DNA to the ends of linear chromosomes as a means of solving the end replication problem, preventing non-homologous end joining, and eliminating inappropriate DNA damage response. In humans, the G-rich telomeric repeats are bound in a sequence-specific manner by proteins belonging to the shelterin complex. Two of the proteins incorporated in the shelterin complex are POT1 and TPP1. POT1 binds to the single stranded telomeric overhang with high affinity and specificity, and TPP1 forms a complex with POT1 to increase POT1-DNA affinity. The POT1-TPP1 complex has been found to participate in a dual role at the chromosome end, both protecting the integrity of the telomere and engaging in telomerase stimulation.

Oligonucleotide/oligosaccharide binding folds (OB domains) consist of a five-stranded closed beta barrel, and most OB-folds use this folded face for ligand binding or as an active site. The DNA-binding domain of POT1 is composed of two tandem N-terminal OB domains. Interestingly, the N-terminal OB-fold of TPP1 (TPP1-OB) is the domain implicated in the actual act of recruiting telomerase to the telomere via interaction with the telomerase RNA and/or TERT protein; this interaction could be direct or indirect. The goal of this work was to elucidate what surface of TPP1-OB is responsible for the recruitment interaction with telomerase, and then to examine what element, if any, in the telomerase RNA subunit is interacting with TPP1. Studying the mechanisms of telomerase access to the telomere is essential for understanding normal biological processes, like aging, as well as comprehending the mechanistic cause of diseases like aplastic anemia, dyskeratosis congenita, cancer, and idiopathic pulmonary fibrosis.

Acknowledgements

I would like to thank the entirety of the Cech Lab, both past and present members, who have been so helpful and supportive throughout my time here. I always enjoyed coming into lab and getting to learn something new and helpful from each scientist. Every single person was always so eager to teach, and getting to know such amazing individuals over my four years has been more than I could have asked for.

I would like to especially thank Art Zaug, JK Nandakumar, and Dr. Cech. Art was always so helpful in teaching me essential techniques, providing a plethora of experimental materials, and offering a good laugh (as long as I was in the lab before noon). JK was the most amazing mentor over my four years in the lab, always relaxed, kind, and funny. I could ask him any questions I had, both of the intelligent and unintelligent variety, and he taught me the majority of what I know regarding basic science research. I would like to thank Dr. Cech for allowing me to have this opportunity and providing guidance through my growth as a scientist. "Tom School" sessions over the summers were priceless, and I have such gratitude for the time he has taken to work with me.

Section 1 – Background and significance

1.1 – The Telomerase Enzyme

The core catalytic components of the telomerase enzyme are the catalytic protein component (TERT) and the RNA component (TR) (1, 2). TERT has a central region that shares homology with viral reverse transcriptase active-site motifs (2, 3, 4), and TR provides the template for repeat synthesis and a catalytically significant pseudoknot/triple helix domain (**Figure 1**)(5, 6, 7). Pseudoknots are secondary structures of nucleic acids in which the hairpin loop of one stem-loop base-pairs with another single-stranded region. TR diverged quickly in evolution, but the RNAs from different organisms share specific structural features like the pseudoknot and template domains (8, 9). TERT and TR are the minimum requirement for telomerase enzymatic activity (1, 2), but *in vivo,* this enzyme is accompanied by several telomerase-associated proteins and factors.

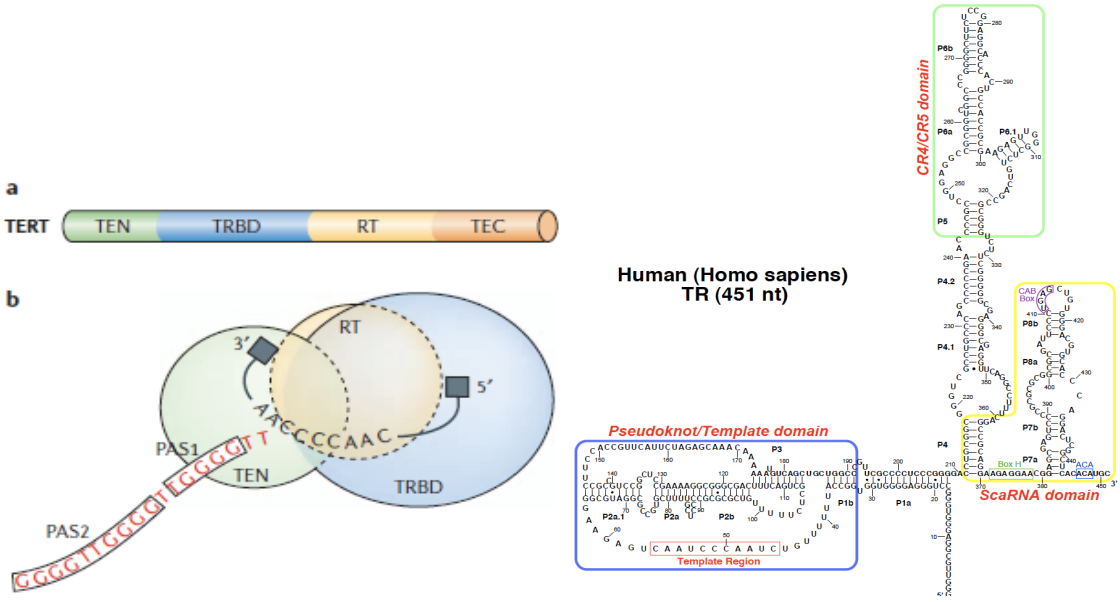

Figure 1 – TERT domains and TR seondary structure. TERT has four domain regions: Telomerase essential N-terminal (TEN) domain, TERT high-affinity RNA-binding domain (TRBD), reverse-transcriptase (RT) domain, and TERT C-terminal (TEC) domain. TR is 450 nucleotides, and has highly evolutionarily conserved elements highlighted (Figure from (51, 52)).

Ribonucleoprotein (RNP) biogenesis, in which TERT and TR come together to form an active complex, is tightly regulated. In human cells, RNA polymerase II transcribes TR, which is then capped on its 5' end and processed at the 3' end (10, 11, 12). The 3' domain of TR contains both a Cajal body localization sequence and an H/ACA motif. Cajal bodies are sub-organelles in the nucleus of cells that are actively dividing and found to function in RNA-related metabolic processes like RNP biogenesis. A complex of four proteins (dyskerin, GAR1, NHP2, and NOP10) associates with small nucleolar RNAs (snoRNAs) to form H/ACA-motif RNPs. The role of snoRNAs is to guide other RNAs through modifications, like methylation or pseudouridylation, by binding protein molecules to form modifying snoRNPs. As RNA polymerase II is transcribing the TR gene, H/ACA-motif RNP proteins are binding and assisting in processing activities (13, 14, 15). While TR itself is structurally considered a snoRNA, it steers clear of modifications and (unlike other snoRNAs) contains a Cajal body localization sequence. TR has largely been found to accumulate in Cajal bodies (16, 17) via the interaction of its Cajal body localization sequence

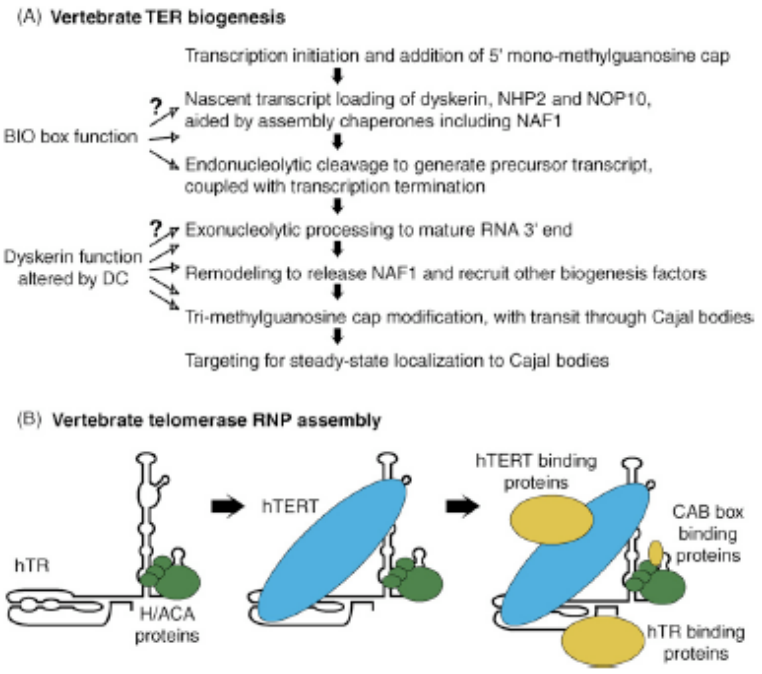

Figure 2 – Telomerase enzyme biogenesis pathway. (A) A series of biochemical steps leads to the generation of the mature telomerase RNA. (B) An ordered assembly with TR and H/ACA proteins, TERT, and various TERT binding proteins then occurs to form the full holoenzyme in the Cajal bodies (Figure from (18)).

(that is found in RNAs known as scaRNAs) with TCAB1 (18). TERT, which is transcribed and translated via conventional pathways, can then bind the RNA and form the telomerase complex or holoenzyme in the Cajal bodies (**Figure 2**).

Telomerase at chromosome ends is able to add repeats of six DNA bases, GGTTAG in humans, using a small portion of its RNA as a template. Telomerase can then either let go of its telomeric substrate or translocate to add another six bases (**Figure 3**) (19). The terms used to express telomerase's ability to continue DNA synthesis are nucleotide addition processivity (NAP) and repeat addition processivity (RAP). NAP refers to the probability that the DNA substrate will not dissociate from the enzyme after the addition of each nucleotide, and RAP refers to the probability of continued utilization of the growing primer during the translocation step after the end of the template is reached (20).

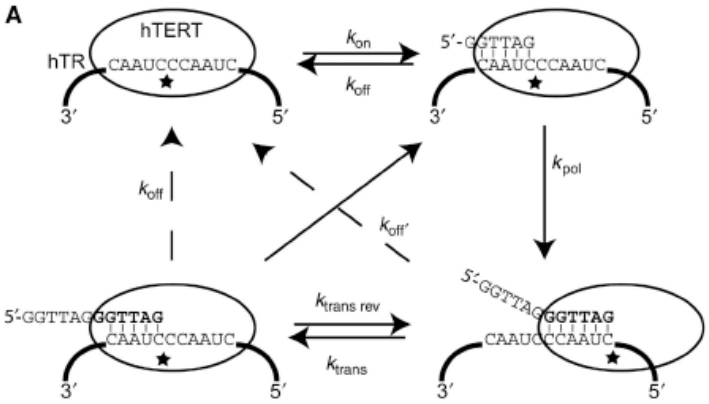

Figure 3 – The telomerase catalytic cycle and its associated rate constants. Association of telomeric DNA and telomerase is represented by k_{on}, and dissociation of substrate and enzyme is represented by k_{off}. k_{pol} is the polymerization rate constant, determined by the rate-limiting step of DNA polymerization. k_{trans} and $k_{trans\ rev}$ represent the rate of translocation and its reverse rate respectively, and $k_{off'}$ is the dissociation of telomerase from DNA primer substrate after a round of extension (Figure from (49)).

1.2 – The Shelterin Complex

Telomeric DNA in mammals associates with a six-protein complex called shelterin. This complex is essential for distinguishing natural chromosome ends from DNA breaks, preventing DNA repair mechanisms, and regulating the access of telomerase to the telomere (21).

Telomeric Repeat binding Factors 1 and 2 (TRF1 and TRF2) bind the double-stranded telomeric repeats TTAGGG, while Protection Of Telomeres 1 (POT1) can bind the repeats on the 3' ssDNA overhang. TRF1 and TRF2 are able to recruit the other components of the shelterin complex (POT1, Rap1, TIN2, and TPP1), forming a stable complex (**Figure 4**)(22).

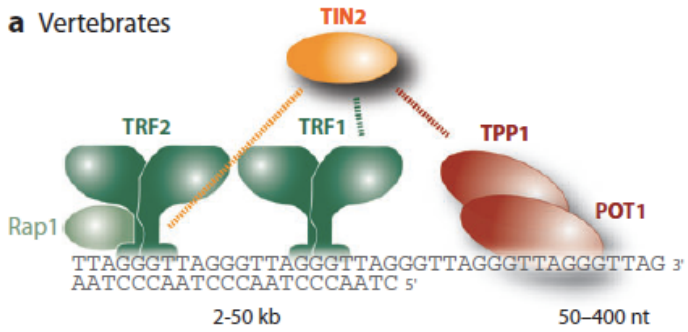

Figure 4 – Depiction of the vertebrate shelterin complex interactions at the telomere. TRF2 and TRF1 bind the DNA duplex, while POT1 binds the single-stranded 3' overhang. TIN2 serves as a central protein in the shelterin architecture. Several of these complexes would coat a telomeric chromosome end (Figure from (39)).

TRF1 and TRF2 – The two proteins share common domain structure, and each has dimeric binding ability that improves its sequence-specific affinity for DNA (23). Their affinity also allows them to act as telomeric architectural factors; TRF1 can loop and pair stretches of telomeric DNA, and TRF2 can form t-loop structures with a telomere substrate (24). Each protein also has a versatile docking domain that serves to recruit other proteins and specific factors to the telomere, a key function of both TRF1 and TRF2 (25).

Rap1 – Rap1 binds TRF2 on the telomere, and is dependent on this interaction for localization to the telomere and stability. Mammalian Rap1 does not have the ability to bind DNA, so its presence in the complex is entirely based on this interaction (26, 27). Other than its associations within the shelterin complex, it is a poorly characterized protein.

TIN2 – TIN2 resides in a central position in the shelterin complex by being able to bind TRF1, TRF2, and TPP1. Therefore, the deletion of TIN2 results in a destabilized shelterin

complex (28). TIN2 is responsible for the recruitment of TPP1 to the telomere as well (29). The interaction of TIN2 and TPP1 is also implicated in the recruitment of telomerase to the telomere, and will be discussed more in depth later (30).

TPP1 – TPP1's C-terminal domain interacts with TIN2, its POT1 binding domain binds the POT1 shelterin protein, and its N-terminal domain contains an OB-fold (TPP1-OB) that is implicated in interacting with telomerase (**Figure 5**)(31, 32, 33). This is part of what indicates a potential role of TPP1 in recruiting telomerase. It has also been shown that the presence of TPP1 helps to recruit POT1 to the telomere and assist in telomere end-protection in the presence of POT1 (34), and the depletion of TPP1 leads to the removal of all detectable POT1 from telomeres and a diminished quantity of POT1 in the nucleus. The absence of TPP1 in the cell also leads to telomere deprotection and shortened telomere length phenotypes (31, 32, 34).

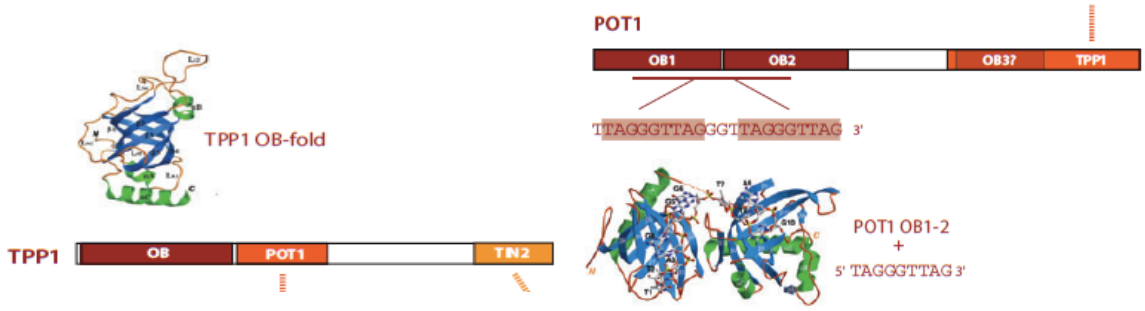

Figure 5 – Structural domains and interactions of TPP1 and POT1. TPP1 interacts with both POT1 and TIN2; its OB-fold structure is shown. POT1 binds TPP1 and single-stranded DNA with its OB-folds, which are structurally depicted (Figure from (39)).

POT1 – POT1 has two OB-folds in its N terminal-region that bind the single-stranded telomeric overhang, and a C terminal domain that binds TPP1 (**Figure 5)**(35). Structural analysis has indicated that there is conservation between POT1 and TPP1 in mammals and TEBPa and TEBPb in ciliates, and the DNA binding preferences for POT1/TPP1 and TEBPa/b are analogous (**Figure 6**)(36).

POT1 prefers binding TAGGGTTAG at the 3' end, and binding affinity is enhanced by TPP1 (36). Similarly TEBPa forms a tight cap over the 3' end of ciliate telomeric DNA and this interaction is enhanced upon heterodimerization with TEBPb. The partial access to the telomere imparted by the POT1-TPP1 complex has been explored further with regard to telomerase interacting with its telomeric substrate.

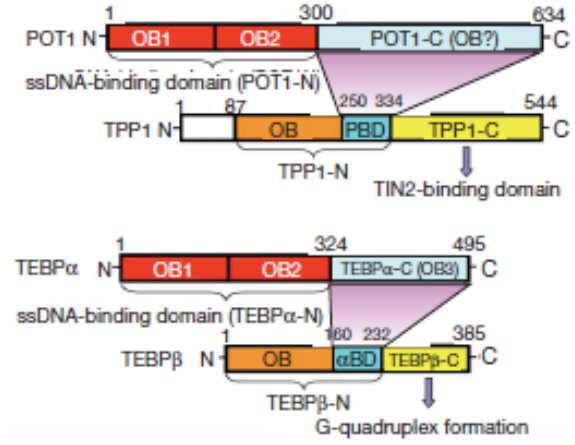

Figure 6 – Human POT1-TPP1 and *O. nova* TEBPa-TEBPb have similar structure and domain function. POT1 and TEBPa both have two OB folds that bind single-stranded telomeric DNA, and a C-terminal domain that binds to its respective partner. TPP1 and TEBPb both have N-terminal OB-folds and central domains that have corresponding binding to the partner protein. Numbers represent the number of amino acids from the N-terminal end (Figure from (36)).

1.3 - The Telomere Structure and Function

Double-stranded telomeric repeats terminate in guanine-rich 3' ends and cytosine-rich 5' ends. The length of the telomeric repeat tracts in mammals has great variability; human telomeres are 10-15 kilobases (kb) while laboratory mice telomeres are 20-50 kb (37, 38). The great variability in lengths across organisms and single cells, and the great variability of experimental results, has made it difficult to ascertain a critical length of telomeres necessary to prevent senescence or chromosome end fusion events (39). The actual end structure of the mammalian

telomere is not blunt, but instead has a 3' overhang (40, 41). The 5' end has a specific sequence ATC-5', but this specificity is lost in the absence of POT1; end specificity is thought to be generated either by POT1 protecting a portion of the DNA or POT1 recruiting a nuclease to the telomeric end (41). This terminal structure has further been found to organize into a lariat structure called a t-loop, formed through a DNA duplex invasion by the 3' overhang, displacing the 3' strand. T-loops are proposed to provide telomere protection by concealing the ends from DNA repair machinery (**Figure 7**)(42).

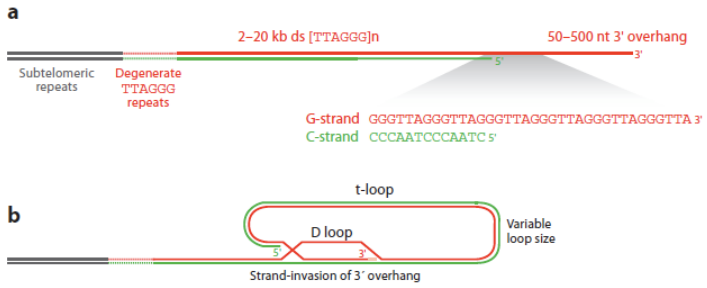

Figure 7 – Human telomere and telomeric structure. (A) The ends of chromosomes have subtelomeric repetitive elements, followed by degenerative TTAGGG repeat elements. The length of the telomere will vary, as will the termination point of the 3' end. The 5' end always ends with ATC-5'. (B) The t-loop structure of the telomere, showing strand invasion of the 3'-overhang, and the formation of a D loop (Figure from (39)).

Telomeres are essential for preventing the activation of DNA damage responses. ATM and ATR kinase pathways alert cells to genomic integrity problems, where the ATM pathway responds to double-stranded breaks and the ATR pathway responds to single-stranded formations. These kinases phosphorylate histone H2AX, leading to the local accumulation of DNA damage response factors, like MDC1 and 53BP1, and the creation of DNA damage foci. The phosphorylation cascades eventually inhibit cell cycle progression and activate p53 (43). Double-stranded breaks in DNA are often repaired by nonhomologous end joining (NHEJ) and homology directed repair (HDR), which are two mechanisms that compromise chromosome termini. DNA damage response at telomeres is

prevented because TRF2 represses ATM activation, whereas POT1 prevents activation of ATR (48).

The presence of telomeres evades these senescence pathways and maintains genome integrity by distinguishing chromosome ends from damage sites. Additionally, telomerase circumvents the DNA end-replication problem. The end-replication problem arises because of the DNA polymerase requires a 3'-OH group for nucleotide addition. As a result, DNA polymerases cannot initiate synthesis without an RNA primer. These primers are degraded and replaced by DNA, but the last RNA primer on the lagging strand cannot be replaced by DNA after its removal (44). This means that after every round of replication there is a loss of terminal DNA and a shortening of telomeres over time. After a cell has aged and divided many times the telomeres shorten and no longer provide protection. DNA damage response pathways will then be expected to occur, ensuring that aged cells and cells with cancerous potential are eliminated from an organism.

1.4 - The Telomerase Interaction with the Telomere

The catalytic components of telomerase can easily extend a single-stranded telomeric DNA primer on their own, without the presence of shelterin complex proteins (1). In the cell, however, the telomere exists as a complex and dynamic nucleoprotein structure. The shelterin complex plays a pivotal role in determining telomerase's ability to extend its telomeric substrate. Regardless of the telomeric DNA length variation within an individual organism, average telomere length in telomerase-positive cells is maintained in a particular range, implying a balance between telomere attrition and telomere elongation. This balancing act is due to *cis* inhibition of telomerase by the telomeric proteins in the shelterin complex (45). The longer the telomere is, the more protein will be bound to the chromosome end, and the shorter the telomere

is, the less protein will be bound to the chromosome end. Because the shelterin complex is acting as an inhibitor, the shorter telomeres will be preferentially lengthened by telomerase because of their relative lack of inhibitor. Once lengthened by telomerase, the association of more inhibitor decreases the probability of further elongation (46).

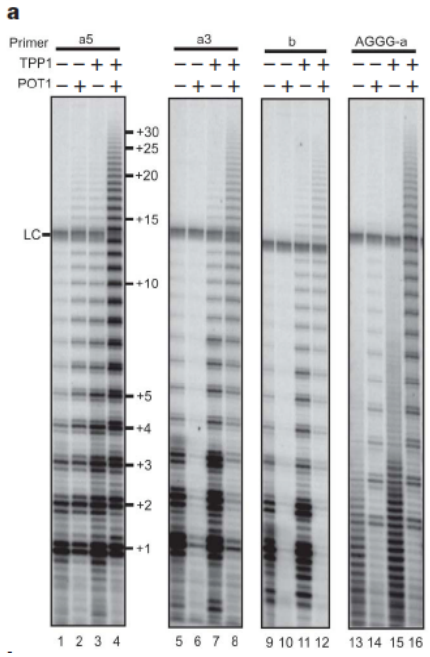

Figure 8 – Direct telomerase activity assay. Direct assays demonstrate that POT1-TPP1 enhances telomerase processivity. The assays used 100nM primer in the presence of POT1, TPP1, or POT1 and TPP1. With primer a5, the addition of either protein shows some RAP stimulation, but the addition of both proteins shows significant stimulation of RAP (Figure from (36)).

The POT1-TPP1 shelterin subcomplex has been identified as playing a central role in telomerase access to the telomere, binding the guanosine-rich 3' overhang with specificity and nanomolar affinity (35, 47). POT1-TPP1 has predominantly been thought to prevent telomerase from accessing the telomere. When deleting either protein *in vivo*, telomere deprotection phenotypes and the lengthening of the telomere in telomerase positive cells are observed (31, 32, 33). The absence of POT1 or TPP1 also leads to DNA damage response signaling pathways discussed previously (41, 48). When POT1-TPP1 is not bound at the very 3' end of the DNA, but instead is bound upstream leaving a 3'-extension of 6 – 8 nt, it can play a role in positive regulation of telomere extension. The dimer promotes repeat addition processivity (RAP) in direct primer extension assays *in vitro* when forced to bind at a slightly internal site on the primer (**Figure 8**)(33, 36). The binding of POT1-TPP1 to a DNA primer inhibits its dissociation from telomerase during active polymerization cycle, and increases the

efficiency of the translocation step, either by slowing primer dissociation or through an independent dimer contribution (49).

These observations indicate a functional interaction between DNA-bound POT1-TPP1 and telomerase that enhances RAP. A current model for this interaction is similar to a 'fixed clamp,' in which the POT1-TPP1 holds the DNA to telomerase in a transient manner during precarious translocation steps (49). This same study found evidence in support of recruitment, demonstrating that POT1-TPP1 stimulates RAP of telomerase at sub-stoichiometric concentrations (49). Interaction between TPP1 and telomerase in GST-pull down assays has also been reported (**Figure 9**)(33), but because this study used crude extracts, it is not known whether the interaction is direct or indirect. The work demonstrated that the OB-fold of TPP1 was the necessary component for pulling down telomerase, indicating a potential site of interaction that leads to the functional observations regarding POT1-TPP1 and RAP. Looking at this interaction from the telomerase perspective, mutating the Gly100 residue on the N-terminal domain of human TERT disrupted RAP enhancement typically seen by POT1-TPP1 presence (50). This finding is consistent with an interaction between telomerase and TPP1, which once again could be direct or indirect. *In vivo* studies in mouse and human cells have also implicated TPP1 as a player in

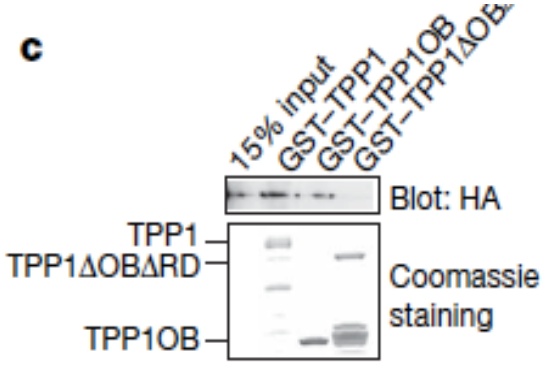

Figure 9 – The TPP1 OB-fold demonstrates interaction with telomerase. GST-tagged TPP1 constructs were used to pull down *in vitro* translated HA-TERT/TR, samples were run on an SDS-PAGE, and presence of telomerase was blotted for with anti-HA antibodies. The full TPP1 protein and the TPP1-OB domain were able to pull down and interact with telomerase. TPP1 without its OB-fold was unable to do the same, implicating TPP1-OB in telomerase recruitment interactions (Figure from (33)).

telomerase recruitment. Visualized through fluorescence in situ hybridization (FISH) and chromatin immunoprecipitation (ChIP), depletion of either TIN2 or TPP1 removes detectable telomerase from the telomeres (30). The study confirms the role of TPP1-OB in telomerase recruitment (**Figure 10**), but demonstrates that the presence of POT1 does not influence recruitment in vivo (30).

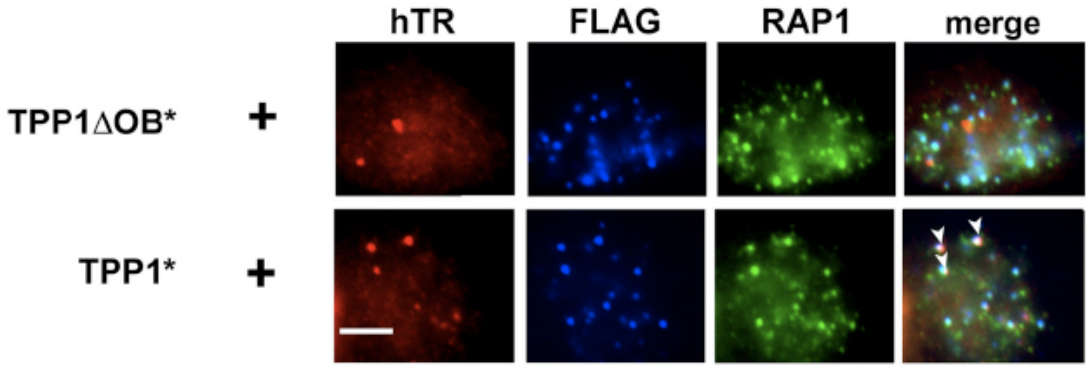

Figure 10 – TPP1-OB domain is required for telomerase RNA localization to telomeres. HeLa cells were transfected with shTPP1 and TPP1ΔOB* or TPP1*. FISH and IF allow visualization of hTR (red), FLAG-tagged TPP1 (blue), and RAP1 (green telomere marker). The superimposition of panels and the fluorescent signals indicates co-localization. TPP1ΔOB* was unable to localize telomerase to the telomere (Figure from (30)).

1.5 – Thesis Aims

As of yet, there is no crystallography data elucidating the nature of the TPP1-telomerase surface interaction. The primary aim of this work was to identify the surface of TPP1-OB responsible for contact with the telomerase enzyme in order to more fully understand recruitment and telomere elongation mechanisms. This was approached using sequence alignments to determine highly evolutionarily conserved amino acid residues on the surface of the OB-fold, and the creation of a series of mutants through QuikChange mutagenesis. Electrophoretic mobility shift assays (EMSA) and filter binding assays were then used to identify TPP1 mutants that do not alter POT1-DNA binding, allowing further work to identify amino acid residues that

solely function to contact telomerase. Mutated residues on TPP1-OB were then tested for their ability to stimulate RAP in direct primer extension telomerase assays, a potential indicator of TPP1-telomerase interaction.

A secondary goal of this project was to examine this interaction from the perspective of the telomerase RNA (TR), trying to identify residues on TR that are contacting TPP1. A similar approach was taken by creating different constructs of TR, mutating both larger RNA tracts and single ribonucleotide residues in the template and pseudoknot regions. The TR constructs with single mutations are known disease mutations in conditions such as aplastic anemia and dyskeratosis congenita. These constructs were tested in the absence and presence of POT1-TPP1 to compare RAP capabilities of telomerase with the goal of garnering information about the telomerase face of this functional interface.

Section 2 – TPP1-OB mutant protein preparation and POT1-DNA binding properties

2.1 – Rationale for mutagenesis screen, cloning and protein preparation

TPP1-OB's potential role in recruiting telomerase to the telomere has been experimentally examined through TPP1-OB pull down of telomerase, and the necessary co-localization of TPP1-OB and TR at the telomere (30, 33). It is still unclear, however, exactly where this contact is occurring on TPP1's OB-fold. The function of telomerase recruitment is a vital, and thus a presumably well-conserved function. The surface of TPP1-OB involved in this interaction in humans is likely to also be involved in the same interaction in many mammalian species, so there should be important evolutionarily conserved residues on the surface of this domain. To determine whether or not there were residues fitting this specification an amino acid sequence alignment was done using many species' TPP1-OB amino acid sequences (**Figure 11a**). The sixteen amino acids highlighted in red were determined to be conserved across species and on the domain surface (**Figure 11b**). Point mutagenesis was used to create fourteen different TPP1-OB mutants (twelve single-mutants and two double-mutants), so the proteins engineered each contained one or two amino acids that potentially play an essential role in telomerase recruitment. A TPP1-N construct (containing TPP1-OB and the POT1 binding domain) was used as the template in the mutagenesis. The TPP1-N construct has been shown to be sufficient for POT1 binding and *in vitro* stimulation of the telomerase extension reaction (36). Both mutant and wild-type Smt3-tagged TPP1-N were grown in bacteria and then purified using a nickel column and fast protein liquid chromatography (FPLC). Final purified samples were run on an SDS-PAGE gel (**Figure 11c**), showing that the amounts and purities of each of the fourteen mutants are comparable to that of wild-type TPP1-N.

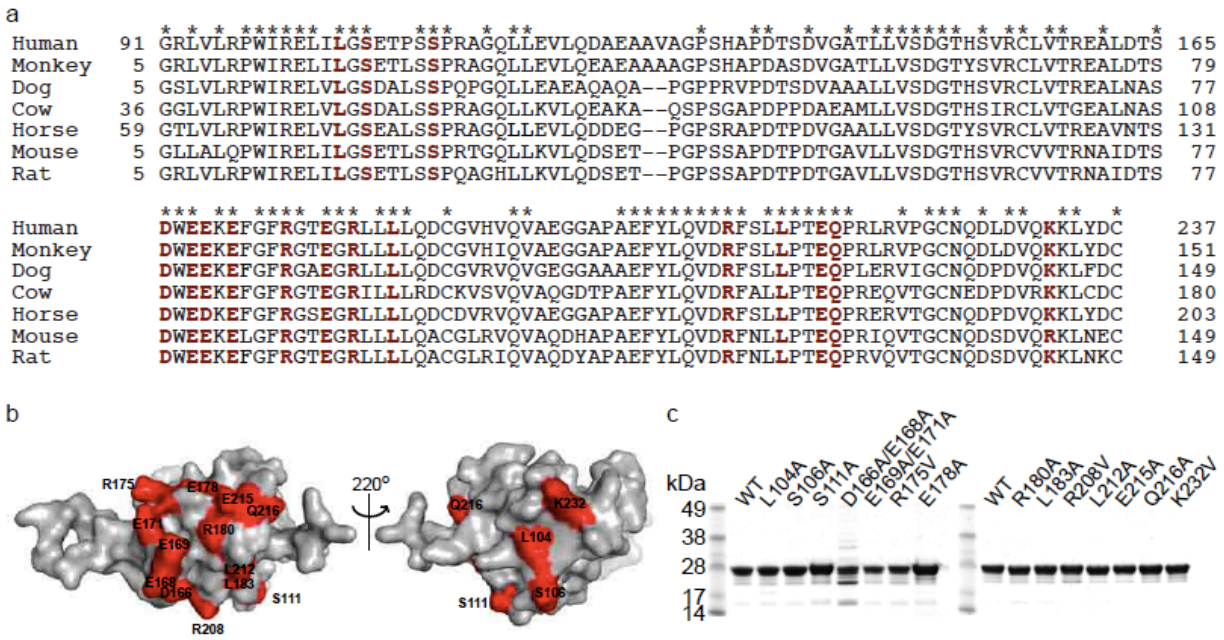

Figure 11 – Evolutionarily conserved surface residues of TPP1-OB as the basis for mutagenesis. (a) An amino acid sequence alignment of TPP1-OB from several different mammalian species. The '*' indicates residues that are highly conserved in the domain, while the elements highlighted in red indicate residues that are both highly conserved *and* on the surface of the domain. (b) Structure of the human TPP1-OB domain with highly conserved surface amino acids highlighted in red. (c) SDS-PAGE gel of 4 µg purified TPP1-N protein and the fourteen TPP1-N mutants descrived herein. The ladder on the left indicates the size of the purified proteins.

2.2 – Testing the ability of TPP1 mutants to bind POT1-DNA and increase POT1-DNA affinity

It was important to make sure that the single mutations made on TPP1-OB were only disrupting the protein's potential telomerase recruitment role and not other functions, like stably binding POT1-DNA or enhancing the affinity of POT1 to bind telomeric DNA. Since the mutations were made on the surface of TPP1-OB, it seemed they would not cause major structural perturbations to the protein. In order to ensure that the single mutations did not disturb the typical ternary complex formed by TPP1, POT1, and single-stranded DNA *in vitro*, an electrophoretic mobility shift assay (EMSA) was performed. The purified TPP1-N, POT1, and a ^{32}P 5'-labeled 20 nucleotide long primer with two telomeric repeats were used. The first lanes show the POT1 protein complexed with the labeled 20 mer oligonucleotide in the absence of

TPP1-N. The addition of TPP1-N (both wild-type and mutants) causes a supershift; the complex shifts to lower mobility on the EMSA, indicating the TPP1-N, POT1, and the labeled DNA have formed a stable complex (**Figure 12a**). This stable complex is formed with wild-type and with each mutant protein made. While there is a defined supershift with each of the mutant TPP1-N constructs, there are noticeable differences in the magnitude of the supershift. This can be accounted for by looking at the charge differences imparted by the amino acid mutations. For instance, mutating an aspartic acid or a glutamic acid (negative) to alanine (neutral) makes the TPP1 protein more positively charged and thus less mobile on the gel. Similarly, mutating arginine (positive) to alanine or valine (neutral) makes the TPP1 protein more negatively charged and thus more mobile on the EMSA. Even with these small mobility differences, the EMSA demonstrates that the purified wild-type and mutant TPP1-N constructs can stably bind with POT1-DNA.

TPP1 has been shown to increase POT1's binding affinity for telomeric DNA (35, 47), so it was necessary to investigate whether or not the mutant TPP1-N constructs demonstrated any deviations in this function. Filter binding assays were used to generate POT1-DNA binding curves and determine dissociation constants for each TPP1-N variation. Increasing amounts of POT1 were added to a constant amount of a ^{32}P 5'-labeled DNA 12 mer; these reactions were either in the presence or absence of TPP1-N (wild-type and mutant variations). The addition of TPP1-N to POT1-DNA consistently increased binding affinity (**Figure 12b**). This increase was seen with the addition of wild-type TPP1-N, as expected, but also with each of the fourteen mutant TPP1-N proteins. Tighter binding affinity is represented by all of the reaction curves shifting distinctively leftward with the addition of TPP1-N (wild-type and mutants), and the

lowering of the calculated dissociation constant values compared to POT1 and DNA alone. This result indicates that the mutations made in the TPP1-OB domain are not affecting normal structure or function of the protein in terms of binding POT1 and enhancing its affinity for telomeric DNA substrates.

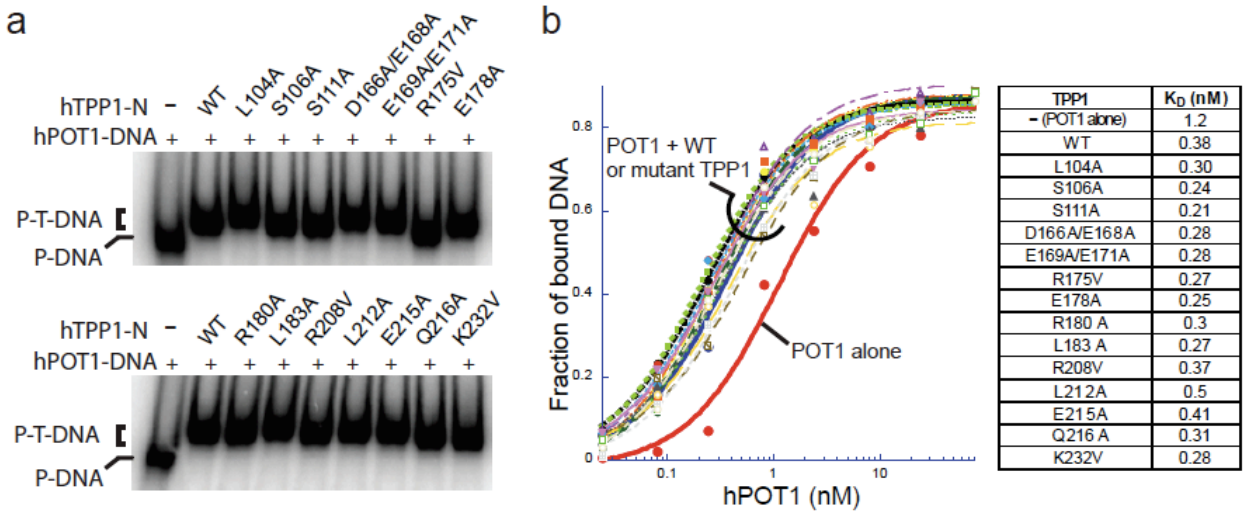

TPP1	K_D (nM)
– (POT1 alone)	1.2
WT	0.38
L104A	0.30
S106A	0.24
S111A	0.21
D166A/E168A	0.28
E169A/E171A	0.28
R175V	0.27
E178A	0.25
R180 A	0.3
L183 A	0.27
R208V	0.37
L212A	0.5
E215A	0.41
Q216 A	0.31
K232V	0.28

Figure 12 – TPP1-OB mutants have wild-type-like function for binding POT1-DNA and enhancing POT1's affinity for DNA. (a) EMSA demonstrating the formation of a stable ternary complex of TPP1-N, POT1, and 5' 32P-labeled oligonucleotide $(dT)_8$GGTTAGGGTTAG. The '-' lane indicates a reaction forming a complex just between POT1 and DNA, while each subsequent lane demonstrates a supershift (and thus a ternary complex) with the addition of each TPP1-N variation. (b) Filter binding assays were performed to test mutated TPP1-N's ability to enhance POT1 affinity for DNA. Trace amounts of 5' ^{32}P-labeled DNA was combined with increasing concentrations of POT1 in the presence or absence of TPP1-N variations. The curves were plotted and analyzed on Kaleidograph (Synergy Software). Dissociation constant (K_D) values were calculated with the equation, Fraction Bound – ([POT1]*m1/([POT1]+K_D)+m3), and the values for each TPP1-N (wild-type and mutants) are shown on the right.

2.3 – Materials and Methods

Site-directed mutagenesis: QuickChange® Site-Directed Mutagenesis Kit from Agilent Technologies was used. Fully complementary mutagenic primers were used to create single mutations in the OB domain of TPP1. The plasmid used was a modified pET28b vector with a

6XHis tag that was fused with a SUMO protein at the N-terminus. 50 µl PCR reactions contained 1 µl pfu polymerase, 5 µl pfu polymerase reaction buffer, 0.5 µl dNTP mix (25 mM each), 40.5 µl Elution Buffer (EB, QIAGEN), 1 µl each of top and bottom primers (15 µM), and 1 µl plasmid (100 ng/µl). PCR cycle program was 1 minute at 95ºC, 45 seconds at 95ºC, 1 minute at 55ºC, 10 minutes at 68ºC (repeat 95-55-68ºC cycle 18 times), 10 minutes at 68ºC, and 4ºC staying temperature. Dpn1 digests were done using 1 µl Dpn1 enzyme, and incubating reactions for 98 minutes at 37ºC. XL10-Gold Ultracompetent Cells were used for transformation and amplification of mutagenized plasmids. DNA was harvested from *E. coli* and purified according to QIAGEN® Miniprep procedures. Isolated plasmids were then sent to Davis Sequencing for confirmation of the desired sequence.

Protein purification: The mutagenized plasmids, each expressing a variation of TPP1, were used to transform BL21(DE3) *E. coli*. Cell cultures were induced for 16 hours with 0.1 mM IPTG at 25ºC. Cells were collected with centrifugation, and cell pellets were resuspended in lysis buffer containing 50 mM Tris-HCl pH 7.0, 500 mM NaCl, 0.2mM PMSF, and 2 Complete lysis tablets. Cells were lysed using sonication, and centrifugation for 1 hour removed cell debris. Supernatant was poured through a column containing 2.5 ml Ni-NTA slurry (QIAGEN) and washed with low concentration imidazole. Protein was eluted off of the column with 2.5 ml of 50 mM Tris-HCl pH 7.0, 500 mM NaCl, 250 mM imidazole. ULP1 protease was added to the elution in order to remove the His-SUMO tag on the protein. Fast protein liquid chromatography (FPLC) was then used to further purify the protein. It was passed through Mono-Q and Superdex200 equilibrated with 25 mM Tris-HCl pH 8.0, 150 mM NaCl. Proteins were concentrated to 1.5-4 mg/ml, flash frozen, and stored at -80ºC. This procedure was performed

for both wild-type and mutant TPP1-N. POT1 used in experiments was made in baculovirus-insect cells prior to this project using procedure described in previous papers (46).

Electrophoretic mobility shift assay (EMSA): Reactions were 10 µl, containing 10 nM 5' ^{32}P-labeled DNA, 20 nM POT1, 40 nM TPP1, 50mM Tris-HCl pH 8.0, 40 mM NaCl, 5 mM DTT, and 6% glycerol. Mixtures were incubated at 4ºC for 30 minutes, then run on a nondenaturing 4-20% gradient polyacrylamide gel (Invitrogen) for 1 hour at 4ºC and 200 V. The gel was dried, and results were visualized using a Phosphorimager (Typhoon Trio).

Filter-binding assays: These assays were performed using a 96-well dot blot box. 23 µl of 25 pM oligonucleotide were put in each well with POT1 at several concentrations (0, .0075, .0225, .075, .225, .75, 2.25, 7.5, 22.5, 75, and 150 nM), 0.1 µg/ml bovine serum albumin (New England Biolabs), 0.1 µg/ml tRNA, 50 mM Tris-HCl pH 8.0, 40 mM NaCl, 5mM DTT, and either buffer or TPP1-N (wild-type or mutant). The 25 µl volume mixtures then sat on ice for 30 minutes. 20 µl of the mixture were then filtered through precooled and dampened membranes on the box. The membranes were previously placed at 4ºC and dampened with 90 µl of cold 50 mM Tris-HCl pH 8.0, 5 mM DTT. This sandwich consisted of a nitrocellulose membrane, a Hybond membrane (positively charged), and filter paper. After the mixtures were filtered through, 20 µl of cold 50 mM Tris-HCl pH 8.0, 5 mM DTT were used to wash the membranes again. Once membranes were dry, the PhosphorImager was used to visualize and quantify the experiment. Analysis involved using Microsoft Excel and Kaleidograph (Synergy Software) software. The dissociation constant was found using the equation, Fraction Bound = ([POT1]*m1/([POT1]+K_D)+m3), where m1, m3, and K_D are numerical parameters used to optimize a curve that best fits the data.

Section 3 – Direct telomerase extension assays demonstrate the effects of TPP1-OB mutations on telomerase processivity

3.1 – Several TPP1-OB mutants elicit defects in telomerase processivity stimulation

The POT1 and TPP1-N complex has been shown to increase the activity of human telomerase by about a factor of two, and increase telomerase processivity by 2-3 fold (36). Since the OB domain of TPP1-N has been implicated in interacting with telomerase and recruiting telomerase to the telomere (30, 33), it is possible that the TPP1-OB domain is required for telomerase activity and processivity stimulation *in vitro*. To test this, the fourteen mutants of TPP1 (which were shown to be otherwise structurally and functionally normal) were used in direct telomerase extension assays with primer a5 (**Figure 13a**). Primer a5 (TTAGGGTTAG**C**GTTAGGG) contains a POT1 binding site at the 5' end and a telomerase-extendible tail at the 3' end. Reactions were allowed to proceed for a designated amount of time, extending the primers with occasional incorporation of radioactive deoxyguanosine triphosphate, and then visualizing the extension products on a sequencing gel. The intensity of the signal can be compared between lanes. Reactions containing both POT1 and wild-type TPP1-N (lane 3) compared to reactions containing neither protein (lane 1) or just POT1 alone (lane 2) demonstrate the same 2-3 fold activity and processivity increase by POT1-TPP1 seen in previous direct telomerase assays (36).

Comparing the reaction containing POT1 and wild type TPP1-N (lane 3) with reactions containing POT-1 and a TPP1-OB mutant (lanes 4–17) helps examine how deleterious certain mutations are to the typical TPP1-induced stimulation. This additionally reveals which surface residues might be important for interacting with telomerase. Figure 1a is one of four sequencing gels, each representing an independent set of reactions. Eight of the mutants [L104A (lane 4), D166A/E168A (lane 7), E169A/E171A (lane 8), E178A (lane 10), R180A (lane 11), L183A

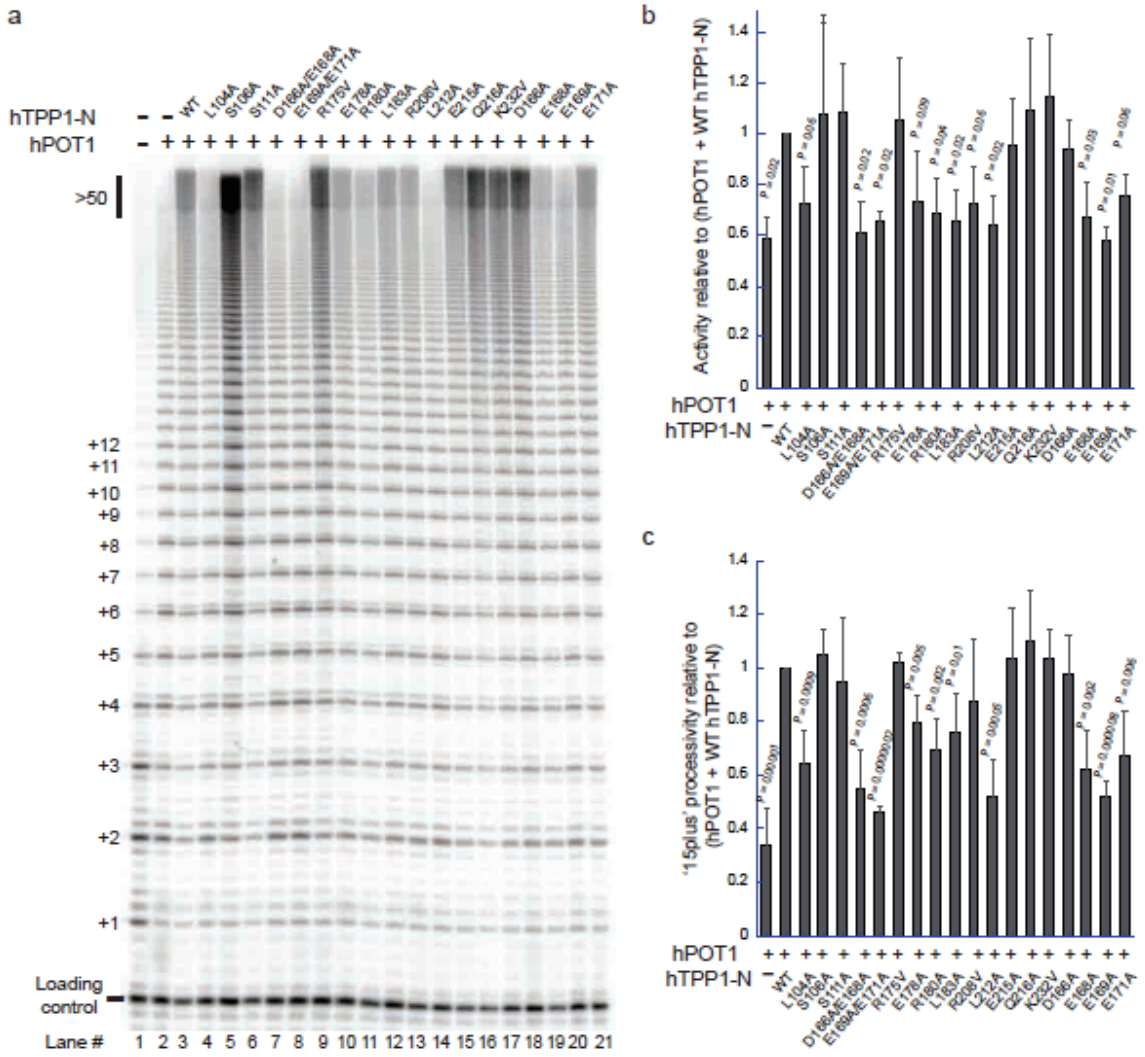

Figure 13 – Particular TPP1-OB mutants show a defect in enhancing telomerase activity and processivity *in vitro*. (a) A representative direct telomerase extension assay using POT1, TPP1-N, and telomerase from HEK293T cell extract. The primer used is a5 at 50 nM. The first lane contains neither POT1 nor TPP1, the second lane contains only POT1, and the third lane contains POT1 and wild-type TPP1-N. Each subsequent lane contains a particular mutant TPP1-N protein. The loading control and each hexad repeat are labeled on the left side. (b) Mean total activity from four independent sets of the assay. Activity is represented by the total band intensity in each lane. The loading control is used to account for loading differences between the lanes. Data is normalized to the reaction using POT1 and wild type TPP1-N, seen in Lane #3. Each lane is shown on the bar graph with standard deviation error bars. A two-tailed t-test was performed on the data set to determine p values for mutants showing significant defective differences from the mutant R175V, which consistently behaved like wild-type. (c) Mean repeat addition processivity from four sets of the assay. Processivity is greater in lanes with a greater ratio of high repeat bands to low repeat bands; this bar graph shows data collected using the '15plus' quantification method. Data is normalized to the reaction using POT1 and wild type TPP1-N, seen in Lane #3. Each lane is shown on the bar graph with standard deviation error bars. A two-tailed t-test was performed on the data set to determine p values for mutants showing significant defective differences from the mutant R175V, which consistently behaved like wild-type.

(lane 12), R208V (lane 13), and L212A (lane 14)], when compared to the use of wild type TPP1-N, show a lower level of total intensity in the lane and fewer high molecular weight bands. A lower total intensity indicates a decrease in telomerase activity, while fewer high molecular weight products indicates lower telomerase processivity. The other six TPP1-N mutants [S106A (lane 5), S111A (lane 6), R175V (lane 9), E215A (lane 15), Q216A (lane 16), and K232V(lane 17)] consistently behaved like wild-type TPP1-N in their stimulation of telomerase activity and processivity. Quantification of telomerase activity (**Figure 13b**) shows that reactions using the defective group of mutants only have 60-70% the activity of wild-type. Similarly, reactions using the defective group of mutants have levels of telomerase processivity 65-80% the processivity of wild-type (**Figure 13c**). These levels are about the same as reactions with POT1 only (lane 2), in which there is a total absence of TPP1-N protein. Therefore, this defective group of mutants is representative of residues that strongly affect typical telomerase stimulation. Because the wild-type-like group of TPP1-N mutants do not hinder telomerase stimulation, we conclude that the corresponding amino acids on the TPP1-OB surface are not important for TPP1's telomerase stimulation function. The double mutant TPP1-N proteins, D166A/E168A (lane 7) and E169A/E171A (lane 8), demonstrated the most significant defects. In order to determine the contribution of the individual acidic residues towards these defects, single TPP1-N mutants D166A, E168A, E169A, and E171A were made and subjected to direct telomerase extension assays (**Figure 13a**, lanes 18-21). Quantification of these reactions (**Figure 13b, c**) shows that E168A, E169A, and E171A significantly affect TPP1's telomerase stimulation function, while D166A behaves like wild-type.

The ability of the POT1-TPP1 complex to stimulate telomerase activity is due to TPP1 alone (36). In order to determine if the eight mutants significantly defective in telomerase

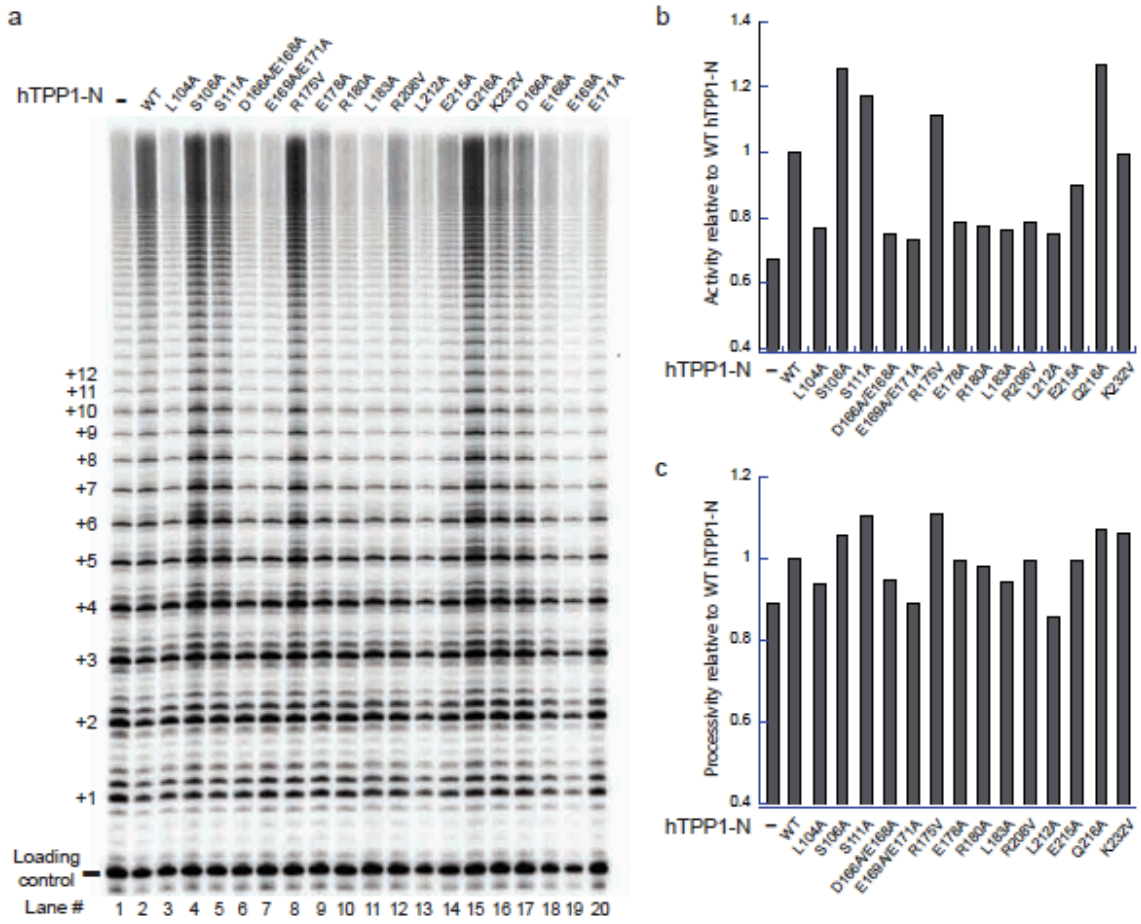

Figure 14 – Particular TPP1-OB mutants are defective in enhancing telomerase activity *in vitro*. (a) A direct telomerase extension assay using telomerase from HEK293T cell extract, TPP1-N protein, and a5 primer at 50nM. The first lane does not contain TPP1-N, the second lane contains wild-type TPP1-N, and each subsequent lane contains a mutant version of the TPP1-N protein. The loading control and each hexad repeat are labeled on the left side. (b) Total activity relative to the reaction with wild-type TPP1-N is shown for each TPP1-N mutant. The loading control is used to account for loading differences between the lanes. (c) Repeat addition processivity normalized to the reaction with wild-type TPP1-N is shown for each TPP1-N mutant. The method of processivity calculation was '15plus.'

processivity stimulation also are defective in telomerase activity stimulation, direct telomerase extension assays were performed with each mutant in the complete absence of POT1. The same cohort of mutants were found to have activity levels about 70% that of wild-type TPP1-N levels (**Figure 14a** and **b**), demonstrating a defect in telomerase activity stimulation. As anticipated, assays in the absence of POT1 did not show significant results regarding telomerase

processivity stimulation (**Figure 14c**). The only difference seen among the aforementioned defective and wild-type-like mutation groups was with mutant E215A, which showed a small 15% decline in telomerase activity. This result suggests a potential moderate involvement of the E215 residue.

To ensure that the effects of the TPP1 mutations on telomerase stimulation are not dependent on the particular primer being used in extension assays, or due to the mutation in primer a5, direct telomerase extension assays were repeated with a different primer. Primer b (GGTTAGGGTTAGGGTTAG) is a purely telomeric sequence that ends in TAG-3'. Previous use of this primer has shown a reduction of telomerase activity in the presence of POT1 without TPP1-N (36), likely because POT1 binds and occludes the 3' end of the primer and prevents extension by telomerase. Reactions that have both POT1 and TPP1-N show an increase in processivity with this primer (36). The same results (**Figure 15a**) of diminished activity with POT1 alone (lane 2) and the subsequent recovery of processivity with addition of TPP1-N (lane 4) were observed. Quantification of reactions with TPP1-N mutants led to similar groupings of defective and wild-type-like TPP1-N variations. The eight TPP1-N mutants that were defective when using primer a5 (L104A, D166A/E168A, E169A/E171A, E178A, R180A, L183A, R208V, and L212A) were also defective in stimulating telomerase processivity with primer b (**Figure 15b** and **c**). E215A, the mutant exhibiting moderate defectiveness, was also compromised in its ability to stimulate telomerase processivity. The results are independent of the primer choice since telomerase activity and processivity stimulation trends were consistent regardless of the primer utilized.

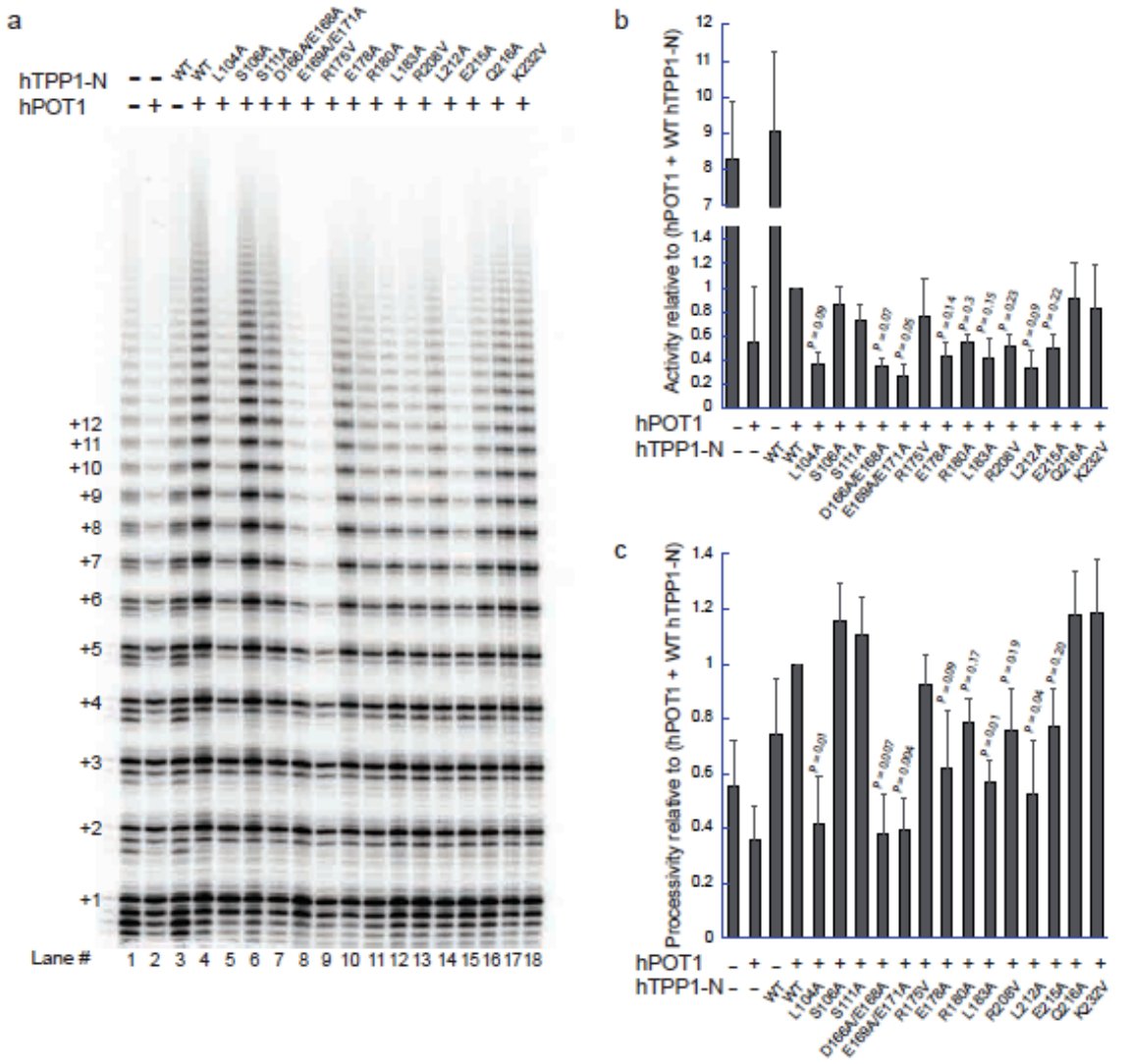

Figure 15 – Effects of TPP1-OB mutants on activity and processivity stimulation *in vitro* using primer b. (a) A representative direct telomerase extension assay using telomerase from HEK293T cell extract, POT1, TPP1-N, and 50 nM primer b. The first lane contains neither POT1 nor TPP1, the second lane contains just POT1, the third lane contains just wild-type TPP1-N, and the fourth lane contains POT1 and wild-type TPP1-N. Each subsequent lane contains a mutant of TPP1-N. The number of added telomeric repeats is labeled on the left side. (b) Mean total activity from three sets of the experiment, normalized to the reaction with POT1 and wild-type TPP1-N. Error bars show the standard deviations, and the significant p values were calculated using a two-tailed t-test comparing other lanes to R175V (a wild-type-like mutant). (c) Mean repeat addition processivity from three sets of the experiment, normalized to the reactions with POT1 and the wild-type TPP1-N. Error bars show the standard deviations, and the significant p values were calculated using a two-tailed t-test comparing other lanes to R175V (a wild-type-like mutant).

3.2 – HeLa cell lines co-expressing TPP1, POT1, and telomerase further demonstrate effects of TPP1-OB mutations on telomerase processivity stimulation

While *in vitro* direct telomerase extension assays shown here and in previous literature show that the presence of POT1 and TPP1 is necessary for telomerase processivity enhancement (36, 49, 50, 53), telomere ChIP and cellular localization studies have conversely shown that POT1 is unnecessary for interaction with telomerase (30). *In vitro* and *in vivo* differences could be due to the artifacts coming from bacterial cell expressed TPP1-N and insect cell expressed POT1. To test the TPP1 mutants for telomerase stimulation in a more physiologically significant setup, we developed a direct telomerase assay that used telomerase, POT1, and full-length TPP1 all synthesized in human cell lines. The HeLa-EM2-11ht cell line uses doxycycline dependent expression of specific genes via a tetracycline promoter. Cell lines were transfected with four different plasmids encoding 3X-Flag-TERT, hTR, 3X-Flag-POT1, and 3X-Flag-TPP1. Mutagenized versions of the 3X-Flag-TPP1 were created using site-directed mutagenesis methods so that several different cell lines were created, each expressing a variation of full-length TPP1 (either wild-type or one of the fourteen mutants) along with the other components. The HeLa-EM2-11ht cells were transfected with the plasmids, allowed to express the genes for 48 hours, and then lysed. These lysates were used for the direct telomerase assays.

Performing direct telomerase assays with primer a5 and 3 µl of the HeLa cellular extracts yields results consistent with what is seen when using bacterially expressed recombinant TPP1 (36). The co-transfection of wild-type TPP1 and telomerase demonstrates an activity stimulation, but not telomerase processivity enhancement (**Figure 14a**). The co-transfection of wild-type TPP1, POT1, and telomerase then demonstrates telomerase processivity enhancement when compared to the over expression of telomerase alone (**Figure 16b**, lanes 1 and 2). Quantification shows the familiar 2 to 3-fold stimulation of processivity (**Figure 16d**), indicating that the effects

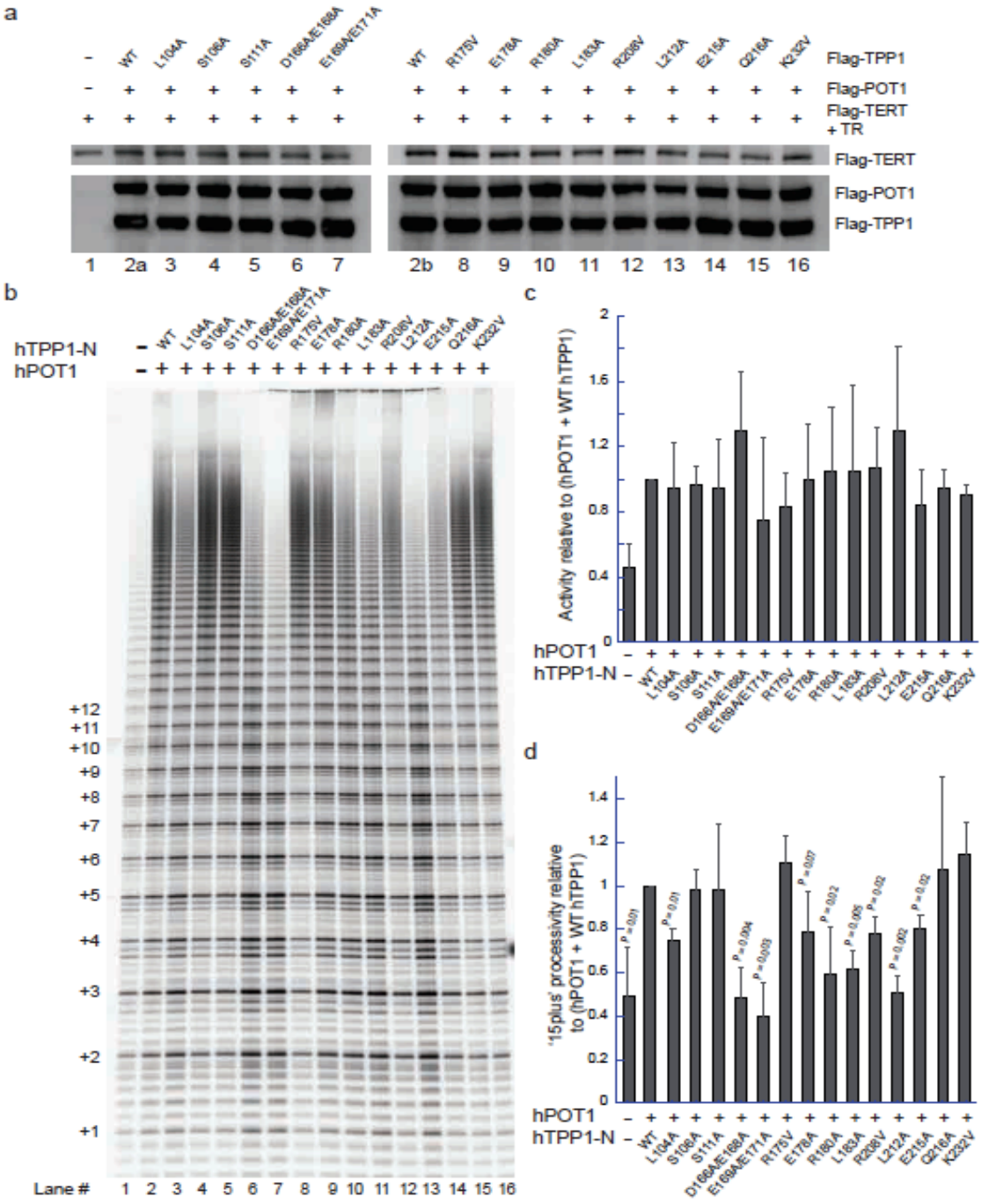

Figure 16 – Direct telomerase extension assay using HeLa cell extracts containing overexpressed POT1, TPP1, and telomerase, reinforce *in vitro* results. (a) Immunoblot of HeLa cell extracts to detect levels of co-transfection for 3X-Flag TERT, TR, 3X-Flag TPP1 (wild-type and mutants), and 3X-Flag POT1. Lysates were probed with an anti-Flag antibody-HRP conjugate. Immunoblot performed by Dr. Nandakumar. (b) A representative direct telomerase extension assay using HeLa cell extracts and primer a5 at 1 µM. The first lane's extract does not contain POT1 or TPP1, while the second lane's extract contains POT1 and wild-type TPP1. Each subsequent lane contains POT1 and a different TPP1 mutant. The number of telomeric hexad repeats is indicated on the left side. (c) Mean total activity of three independent experiments, normalized to the reaction with POT1 and wild-type TPP1. Error bars show standard deviations. (d) Mean repeat addition processivity of three independent experiments, normalized to the reaction with POT1 and wild-type TPP1. Error bars show standard deviations.

of POT1-TPP1 on telomerase are not dependent on the source of POT1 or TPP1 and are not the result of potential artifacts.

Direct telomerase assays were also performed using extracts from co-transfections with telomerase, POT1, and a mutant variation of TPP1. An immunoblot of each transfection was performed, and shows strong and consistent expression of each Flag-tagged protein, including each mutant full-length TPP1 (**Figure 16a**). The results of the direct telomerase assays using extract compared to those using recombinantly expressed protein are very similar. There are substantial defects in processivity stimulation for TPP1 mutants L104A, D166A/E168A, E169A/E171A, E178A, R180A, L183A, R208V, L212A, and E215A, both visually (**Figure 16b**) and when quantitated (**Figure 16d**). E215A, which did not show a processivity defect with primer a5 but did show a defect with primer b, seems to have a moderate defect in processivity enhancement when expressed in the HeLa cell line. Overall, the quantification of this processivity data correlates nicely with the quantification data collected using the bacterially expressed TPP1-N mutants (**Figure 13c**). This indicates that the results collected on important and unimportant mutations in the TPP1 OB domain with regard to telomerase stimulation do not depend on the source of the protein used in telomerase reactions.

Drawing significant conclusions about the effects of TPP1-OB mutations on telomerase activity is more difficult because total activity (unlike processivity) is linearly dependent on the concentration of active telomerase in the cell lysate used. The standard deviations for total activity calculations (**Figure 16c**) are variable and large when compared to standard deviations for telomerase processivity calculations (**Figure 16d**). One potential explanation is that each lane in Figure 4b is essentially an independent telomerase transfection, so total telomerase concentration differences across each of these lanes are 'experimental errors.' Attempting to

normalize with differences in telomerase concentration using the TERT signal of the immunoblot assay (**Figure 16a**) unfortunately does not make accurate corrections.

3.3 – Quantification methodology choice does not impact conclusions drawn

Repeat addition processivity quantification has previously used a method that involves calculating the signal in each and every band of the ladder created by the primer extension reaction (36, 50). When using telomerase generated in rabbit reticulocyte lysate (RRLs), calculating the signal in each and every band of the sequencing gel was a possibility since there seemed to be an upper limit to the amount of primer extension. Using telomerase generated in HEK293T cells or in HeLa cells, however, has been deemed 'super telomerase' because of the significantly higher activity and processivity seen with its use. As was seen in the experiments just described, 'super telomerase' generated high molecular weight products in the extension reactions that were so large they could not be seen as discrete bands on the sequencing gels. Instead, they create a sort of signal smear at the top of each lane. Laboratory members have run these 'super telomerase' reactions on sequencing gels for lengthy periods of time, and have indeed verified that the contents of these smears are discrete reaction products (unpublished data). The previously used 'band counting' methodology no longer seemed appropriate, since it was forced to ignore products that were not identifiable as discrete bands.

The '15 plus' methodology has been used instead to represent the above sequencing gel data. This method, instead of using signal in each and every band, takes a ratio of signals; the signal of 'high molecular weight products' over the total signal (total activity). High molecular weight products are defined as repeat number 15 and over. While this is an arbitrary choice of repeat number, processivity data is always normalized to a particular reaction profile, so all data is relative to a particular standard and conclusions can be drawn from the relative differences.

This method has been preferred for this particular data because it is able to account for the smear of reaction products at the top of each lane, while the other method cannot. Even with this analytical change, data analyzed using the more traditional 'band counting' yields similar quantification results (**Figure 17**). The same implicated group of TPP1-OB mutants are found to be defective in telomerase enhancement.

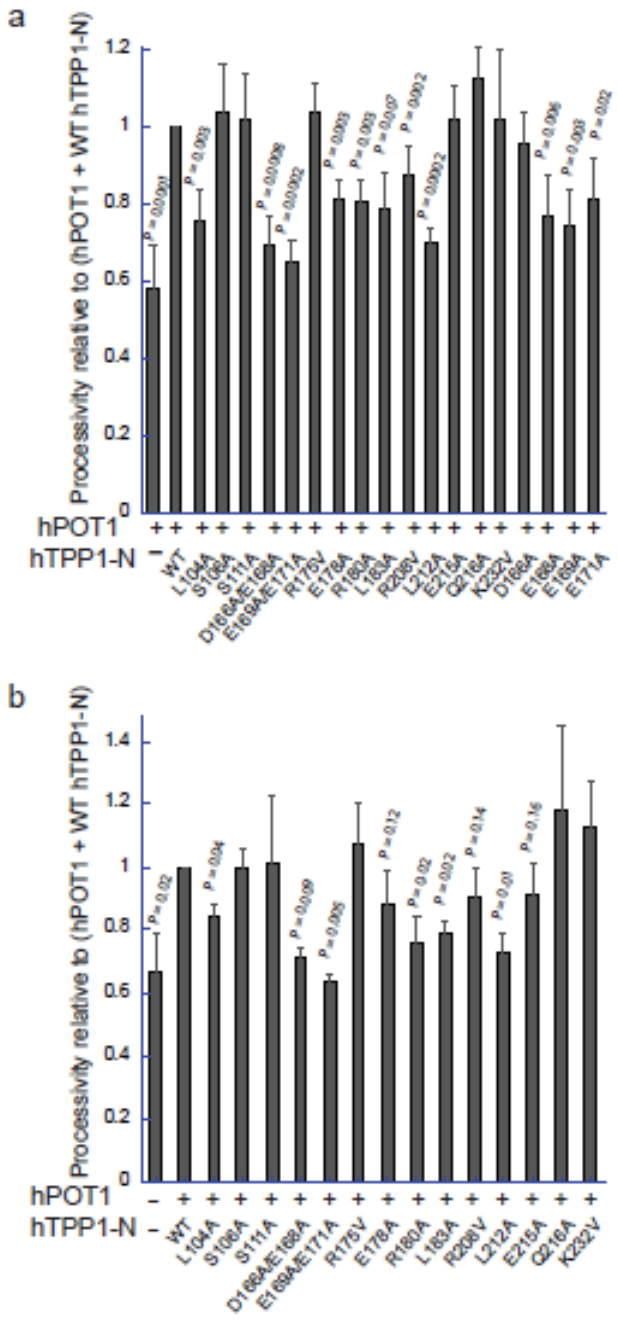

Figure 17 – Repeat addition processivity quantifications of data from gels in figures 1a and 4b using a different methodology of calculation that quantifies individual bands in the sequencing ladder. Due to the extensive overlap and 'smearing' of individual bands of high molecular weight, the '15 plus' methodology was preferred in order to accommodate these bands. (a) Repeat addition processivity quantification of data in figure 1a using 'band counting.' While the other method is preferred, it is important to note the striking similarity of numerical results when compared to the '15 plus' method. (b) Repeat addition processivity quantification of data in figure 4b using 'band counting.' While the other method is preferred, it is important to note the striking similarity of numerical results when compared to the '15 plus' method.

3.4 – Materials and Methods

'Super telomerase' preparation: 'Super telomerase' preparations were in HEK 293T cells, which were transfected with TERT and hTR. The cells were transfected with 4 µg of plasmid DNA and Lipofectamine 2000 (Invitrogen) using 6 well plates and the manufacturer's protocol. Medium used during transfection is OptiMEM without antibiotics. In each well, .66 µg pVan107 (hTERT plasmid) and 3.33 µg pBS-U1-hTR (hTR plasmid) were used. 4-6 hours after transfection, old medium is removed and replaced with OptiMEM with Pen/Strep antibiotics. 24 hours after transfection, cells were trypsinized and transferred to a 25 cm^2 flask. After 24 more hours of growth, cells were trypsinized, washed with PBS, and lysed with 400 µl of Chaps lysis buffer (10 mM Tris-HCl pH 7.5, 1 mM $MgCl_2$, 1 mM EGTA, 0.5% CHAPS, 10% glycerol). Lysate is nutated for 30 minutes at 4ºC, then cell debris is removed with centrifugation for 10 minutes at 4ºC and 13,200 rpm. Supernatant, which is around 4 mg/ml, was quick frozen and stored at -80ºC.

Direct telomerase assay (*in vitro*): 20 µl telomerase reactions contain 50 mM Tris-Cl (pH 8.0), 30 mM KCl, 1 mM $MgCl_2$, 1 mM spermidine, 5 mM beta-mercaptoethanol, .05 µM primer a5 or b, 500 µM dATP, 500 µM dTTP, 2.92 µM unlabelled dGTP, 0.33 µM radiolabelled dGTP (3000 Ci/mmol), and 3 µl of 'super telomerase' cell extract. Reactions containing POT1 and/or TPP1 are at 500 nM of each protein. Reactions are incubated at 30ºC for one hour. Reactions were stopped with 100 µl of 3.6 M ammonium acetate, 20 µg of glycogen, and 5' end-labeled (7.5 cpm/µl) 18 mer loading control. Products were precipitated with ethanol, then washed. Pellets were resuspended in 10 µl H20 and 10 µl loading buffer (95% formamide, 5% H20, loading dye). Samples were heated for 5 minutes at 95ºC for 5 minutes, centrifuged at 13,200 rpm for 10 minutes, and loaded onto a 10% acrylamide (7M urea, 1X TBE) sequencing gel. Gels were run

for 1.75 hours at 90 Watts, dried, exposed to an image plate, and imaged on a phosphorimager (GE). Data was finally analyzed using Imagequant TL software.

Full-length TPP1 site-directed mutagenesis: QuickChange® Site-Directed Mutagenesis Kit from Agilent Technologies was used. Fully complementary mutagenic primers were used to create single mutations in the OB domain of TPP1. The plasmid used was the p3X-Flag-TPP1-Bl4 as the template for PCR. 50 µl PCR reactions contained 1 µl pfu polymerase, 5 µl pfu polymerase reaction buffer, 0.5 µl dNTP mix (25 mM each), 37.5 µl Elution Buffer (EB, QIAGEN), 3 µl DMSO (dimethyl sulfoxide), 1 µl each of top and bottom primers (15 µM), and 1 µl plasmid (100 ng/µl). PCR cycle program was 2 minutes at 96ºC, 1 minute at 96ºC, 1 minute at 60ºC, 10 minutes at 68ºC (repeat 95-55-68ºC cycle 18 times), 10 minutes at 68ºC, and 4ºC staying temperature. Dpn1 digests were done using 1 µl Dpn1 enzyme, and incubating reactions for 98 minutes at 37ºC. XL10-Gold Ultracompetent Cells were used for transformation and amplification of mutagenized plasmids (30 µl of cells, 3 µl of DNA). DNA was harvested from *E. coli* and purified according to QIAGEN® Miniprep procedures. Isolated plasmids were then sent to Davis Sequencing for confirmation of the desired sequence.

HeLa cell transfection and extract preparation: 300,000 cells per well were placed in a 6 well plate and incubated for 42 hours before transfection. Transfections used Lipofectamine 2000 (Invitrogen), 1 µg p3X-Flag-TERT0cDNA6/myc-His C, and 3 µg phTR-Bluescript II SK(+) in each transfected well. Transfections yielding POT1 or TPP1 used 1 µg of p3X-Flag-POT1-Bl4 and 1 µg p3X-Flag-TPP1-Bl4. Control transfections (transfections without POT1 or TPP1) were performed using an empty pBl4 plasmid. Media was removed after 4-6 hours and replaced with fresh media containing 200 ng/ml doxycycline to induce expression of telomerase, TPP1, and POT1 via a tetracycline promoter. Cell lines incubated for 48 hours, were trypsinized, washed

with PBS, resuspended in CHAPS lysis buffer (contents in paper 16) and 1 µl RNasin plus (Promega). This mixture was nutated at 4ºC for 20 minutes, and then centrifuged for 10 minutes at 13,200 rpm. Supernatant was removed, flash frozen, and stored at -80ºC.

Immunoblot of HeLa cell extracts: Standard western and immunoblot protocols were used. Antibodies and dilutions used were mouse monoclonal anti-FLAG/M2-HRP conjugate (Sigma; 1:10,000), rabbit monoclonal TERT (C-term) antibody (Epitomics; 1:500), mouse monoclonal anti-beta-actin antibody (Sigma; 1:10,000). Secondary antibodies and dilutions used were horseradish peroxidase-conjugated goat antibodies against rabbit IgG (Santa Cruz Biotechnology; 1:10,000) or donkey antibodies against mouse IgG (Jackson Immunoresearch; 1:10,000). Chemiluminescence detection was by ECL plus reagents (GE Healthcare Lifesciences), revealing the primary antibodies. Data was visualized and quantified on a FluorChem HD2 (Alpha Innotech) imaging system.

Direct telomerase assay (*in vivo*): 20 µl telomerase reactions contain 50 mM Tris-Cl (pH 8.0), 30 mM KCl, 1 mM $MgCl_2$, 1 mM spermidine, 5 mM b-mercaptoethanol, 1 µM primer a5 or b, 500 µM dATP, 500 µM dTTP, 2.92 µM unlabelled dGTP, 0.33 µM radiolabelled dGTP (3000 Ci/mmol), and 3 µl of cell extract from HeLa-EM2-11ht. Reactions are incubated at 30ºC for one hour. Reactions were stopped with 100 µl of 3.6 M ammonium acetate, 20 µg of glycogen, and 5' end-labeled (7.5 cpm/µl) 18 mer loading control. Products were precipitated with ethanol, then washed. Pellets were resuspended in 10 µl H20 and 10 µl loading buffer (95% formamide, 5% H20, loading dye). Samples were heated for 5 minutes at 95ºC for 5 minutes, centrifuged at 13,200 rpm for 10 minutes, and loaded onto a 10% acrylamide (7M urea, 1X TBE) sequencing gel. Gels were run for 1.75 hours at 90 Watts, dried, exposed to an image plate, and imaged on a phosphorimager (GE). Data was finally analyzed using Imagequant TL software.

Total activity quantification: Gels were quantitated using the Imagequant TL computer program. Total activity was obtained by getting the total number of counts in each individual lane (not including the loading control), using the 'rolling ball' background correction option in the program (usually at ~200). These numbers were normalized to the counts in the corresponding lane's loading control. For data representation, each lane was then normalized to the total activity of the 'standard' or 'wild-type' lane, which would numerically be considered '1.' Each lane's numerical activity then is representative of its percentage of activity relative to the standard reaction (36).

Repeat addition processivity quantification, 'band counting': Each telomerase-generated band in the ladder was individually quantitated. Counts for a band were then normalized by dividing by the total number of radiolabeled guanosines added to a particular extension product (since more radiolabeled nucleotides are incorporated into longer extension products). For a particular band n, a fraction is calculated by taking the sum of the counts of the other repeats (1-n) and dividing it by the total counts in the lane. The natural log of this fraction was then plotted against the repeat number, generating a plot of points for each individual lane. Each plot is then fit with a linear regression equation, generating a slope m. Points corresponding to repeats 2 to 15 were used to fit the regression equation since repeat 1 tended to have an unusually large number of counts, and repeats above 15 demonstrated significant signal overlap during quantitation. The numerical processivity value is $-\ln(2)/m$. Similar to the methods of data representation for total activity, each lane was then normalized to the processivity value of the 'standard' or 'wild-type' lane, which would numerically be considered '1.' Each lane's numerical processivity then is representative of its percentage of processivity relative to the standard reaction (49).

Repeat addition processivity quantification, '15 plus': This was the preferred processivity quantification methodology because of the high repeat number bands generated when using 'super telomerase.' Instead of getting the signal in each individual band of the ladder, just one basic ratio was taken – the total counts of the lane 15 repeats and above divided by the total activity of the entire lane. More processive reactions generate larger ratios, while less processive reactions generate smaller ratios. Data representation, similar to the other methodologies, normalized the ratios to the ratio of the 'standard' or 'wild-type' lane, which would numerically be considered 'l.' Each lane's processivity value is then representative of its percentage of processivity relative to the standard reaction.

Section 4 – Examining potential interaction sites of telomerase RNA with POT1-TPP1 by manipulating the RNA's pseudoknot and template regions

4.1 – The P1 helix of telomerase RNA does not appear to be an interaction site for POT1-TPP1

While the surface of TPP1 responsible for telomerase-TPP1 interaction appears to have been elucidated, the corresponding surface on the telomerase enzyme remains unknown. Repeat addition processivity is affected by mutating the Gly100 residue on TERT (50), but other mutations made in this paper and in ongoing lab experiments have not shown similar changes in processivity enhancement. Continuing to probe TERT for POT1-TPP1 binding via this mutation methodology no longer appears promising. Unpublished lab pull-down experiments have demonstrated, however, that the interaction of POT1-TPP1 with the telomerase enzyme appears to be RNA-dependent. With this in mind, the focus was shifted to exploring potential association sites for POT1-TPP1 on the telomerase RNA.

Comparison and manipulation of mouse and human telomerase systems has suggested that POT1-TPP1 interacts with the pseudoknot domain of the telomeric RNA. When mixing telomerase and POT1-TPP1 components of mouse and human, it was shown that human POT1-TPP1 could stimulate processivity of complexes with either mouse or human TERT. Mouse POT1-TPP1, conversely, required mouse TERT for processivity stimulation. Furthermore, human POT1-TPP1 could only increase processivity in the presence of the human pseudoknot domain (not mouse) of the telomerase RNA (50). A line of experimentation in the lab then focused on strategically humanizing the mouse TR in an effort to see what humanization mutations would correspond to processivity enhancement. This would indicate potential interaction sites of POT1-TPP1 on the telomerase RNA.

Comparing the mouse and human pseudoknot/template domains (**Figure 18**) reveals that one of the major structural and sequential differences is the presence of a P1 helix in humans

(56). Mice do not have either the P1b or P1a portion of this helix. One of the lab members set out to introduce humanizing mutations to the mouse TR, one of these mutations being the addition of a P1 helix. The mutants were then used in the familiar direct telomerase extension assays in the presence or absence of human POT1-TPP1. She found that the addition of the P1 helix to mouse TR greatly increased the overall telomerase activity in the assays, most likely due to the increased stabilization of the RNA structure in the enzyme. She also found an increase in processivity with the addition of human POT1-TPP1, suggesting an interaction between the protein complex and the P1 helix.

Claiming this interaction, however, still needed more experimental support. To further examine the interaction of human POT1-TPP1 and the TR P1 helix, I began a mutational analysis of the human telomerase RNA's P1 helix. The purpose of this investigation was to see if a deletion or perturbation of P1 in human TR decreases the stimulation of processivity in the presence of POT1-TPP1. The

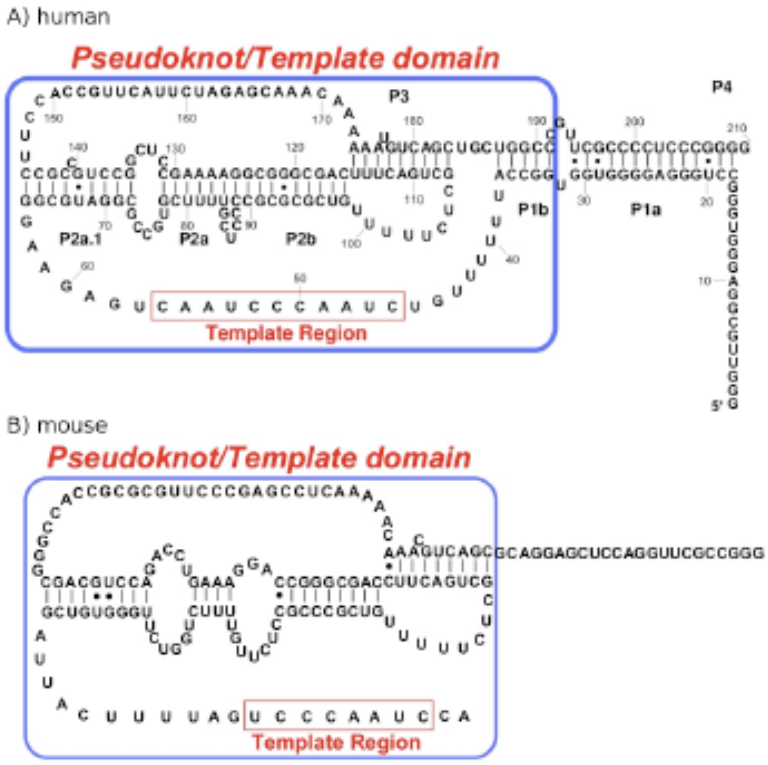

Figure 18 – Pseudoknot domain secondary structures for human TR and mouse TR. (a) Template region of human TR. Compared to mouse (B), it is larger and has additional nucleotides upstream of its template. These extra nucleotides can pair with a sequence downstream to form the P1 helix in human RNA (Figure from (51)).

mutations made involved an hTR construct that was missing its P1a helix (hTR Δ1-32), and a full-length construct of hTR. Using QuickChange mutagenesis, mutations were introduced to the 3' component of P1b (so the strand would not bind), the 5' component of P1b (so the strand would not bind), and complementarily to both the 3' and 5' component of P1b. Mutated plasmids were then used to transform *E. coli*, and amplified DNA was purified with the typical maxi-prep procedures. The six mutated hTR plasmid constructs and wild-type hTR plasmid were each used to transfect HEK 293T cells; each construct was used for two transfections, one in the presence and one in the absence of plasmids for POT1 and TPP1. Lysates of the cell cultures were subjected to direct telomerase extension assays.

As expected, wild-type hTR reactions with the addition of POT1-TPP1 increase both activity and processivity (**Figure 19a**, lanes 1-4). Construct '1' is 3' mutated hTR Δ1-32, '2' is 5' mutated hTR Δ1-32, and '3' is both 3' and 5' mutated hTR Δ1-32 (data not shown). Construct '4' is 3' mutated full-length hTR, '5' is 5' mutated full-length hTR, and '6' is both 3' and 5' hTR. For every mutated construct, the addition of POT1-TPP1 in a direct telomerase extension assay enhanced both activity and processivity (**Figure 19a**, lanes 5-18). If the P1 helix was the direct interaction site of POT1-TPP1 for telomerase processivity enhancement, perturbations of the helix would result in an inability for POT1-TPP1 to result in an enhancement. The interruption of the P1b helix in constructs '4,' '5,' and '6,' did not result in a disruption of processivity enhancement (**Figure 19b** and **c**). The presence of POT1-TPP1 in reactions with each of the constructs results in a definitive increase in both activity and processivity, indicating that the P1 helix is most likely not the site of POT1-TPP1 interaction. The processivity enhancement seen with the addition of a P1 helix to mouse TR could be heavily reliant on the stability imparted by the P1 helix structure. This stability, instead of just increasing activity of the enzyme, may be

allowing telomerase to more easily clear the rate-limiting steps of its catalytic cycle and thus result in processivity enhancement.

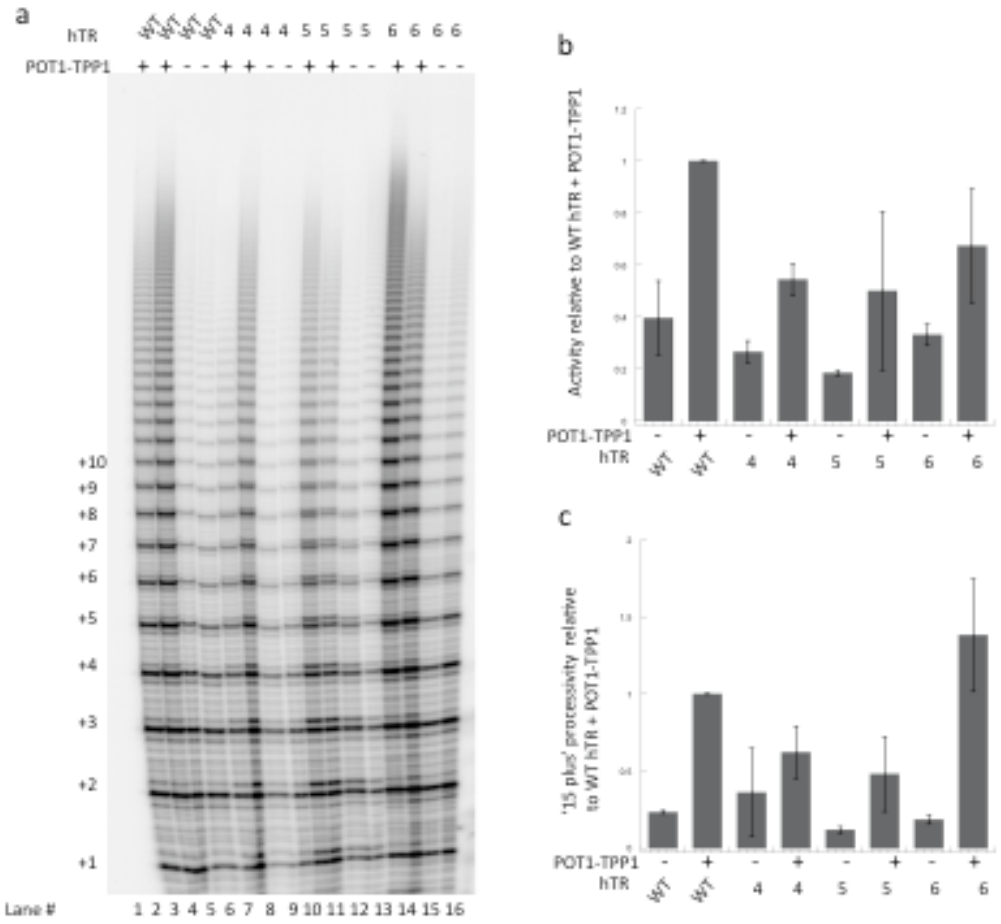

Figure 19 – The P1b helix is not important for POT1-TPP1 stimulation of processivity. (a) A direct telomerase extension assay using HEK 293T cell extracts and primer a5 at 1 μM. Two independent sets of the same reactions are shown on this gel. The extracts contain wild-type hTR or a mutated version of the RNA, each construct either in the presence or absence of POT1-TPP1. The number of telomeric hexad repeats is indicated on the left side. (b) Mean total activity of these two independent experiments, normalized to the reaction with wild-type hTR and POT1-TPP1. Error bars show standard deviations. (c) Mean repeat addition processivity of two independent experiments, normalized to the reaction with wild-type hTR and POT1-TPP1. Error bars show standard deviations.

4.2 – Single nucleotide disease mutations in telomerase RNA cannot demonstrate a POT1-TPP1 interaction with the hTR template/pseudoknot region

Even though manipulation of the telomerase RNA P1 helix proved inconclusive, there are still strong indications that the POT1-TPP1 complex is interacting with the RNA pseudoknot/template domain. The observation that human POT1-TPP1 can only enhance processivity in the presence of a human pseudoknot/template RNA domain still holds true (50), as does the observation that the POT1-TPP1 pull-down of telomerase is RNA-dependent. There are also a plethora of small nucleotide mutations in the pseudoknot/template domain that have been found in patients with aplastic anemia, dyskeratosis congenita, and idiopathic pulmonary fibrosis (**Figure 20**). These mutant versions of telomerase have been shown to be functionally deficient in terms of normal enzyme activity and processivity (57, 58, 59, 60), but it has not been explained why mechanistically at the telomere these mutants are so detrimental. One hypothesis is that the mutations cause an inability for the POT1-TPP1 complex to interact with the telomerase enzyme as it normally would.

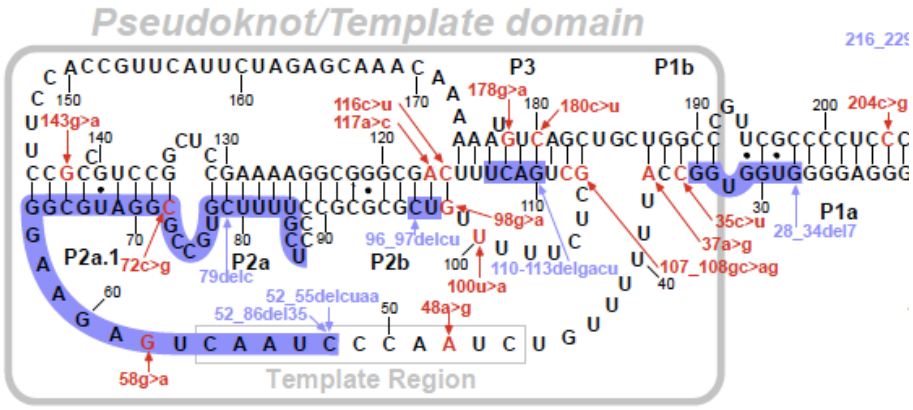

Figure 20 – Autosomal dominant disease mutations found in the pseudoknot domain of human telomerase RNA. Several specific disease mutations, indicated in red, have been identified in the pseudoknot and template domain of hTR. Single mutations such as these can lead to aplastic anemia, dyskeratosis congenita, and idiopathic pulmonary fibrosis in patients (Figure based upon (57, 58, 59, 60)).

To investigate this possibility, a similar mutational strategy was taken with the telomerase RNA. A panel of fourteen mutagenized hTRs were created based upon observed disease-associated mutations. The fourteen base pair changes are as follows, referred to as mutants 1 thru 14 in figures: G58A, C72G, C79del, U100A, GC107-8AG, C116U, A117C, G143A, G178A, C180U, CCACC148-52GGTGG, AGCAAA164-69TCGTTT, G178A, and U101A/G143A. QuickChange mutagenesis methods were again used to engineer each mutated hTR plasmid version. Isolated and sequenced mutant plasmids were then each used in HEK 293T cell transfections (alongside wild-type hTR) either in the presence or absence of POT1 and TPP1 plasmids. Important components of the lysate were immunoprecipitated on FLAG beads, which were then used in direct telomerase extension assays with primer a5 to examine activity and processivity changes.

As expected, wild-type hTR demonstrated a processivity enhancement with the addition of POT1-TPP1 to the reaction (**Figure 21a**, compare lanes 1 and 16). Total activity stimulation seemed to be a more variable measure as has been seen in previous direct telomerase extension assays. Much of the lack of stimulation between mutants could be attributed to their 'catalytically dead' nature before the addition of POT1-TPP1 (**Figure 21b**). The higher activity of wild-type hTR in the absence of POT1-TPP1 may be due to differential protein concentrations (will have to wait for western). For each and every mutant, however, the addition of POT1-TPP1 led to a marked increase in processivity of the enzyme (**Figure 21c**). Wild-type hTR demonstrated about a 1.5-fold increase in processivity, and each of the mutant telomerase variations show a comparable increase in processivity when comparing each construct in the absence and presence of POT1-TPP1 (**Figure 22**). The increase in processivity for each mutant construct suggests that POT1-TPP1 is still able to interact with the mutated telomerase RNA well

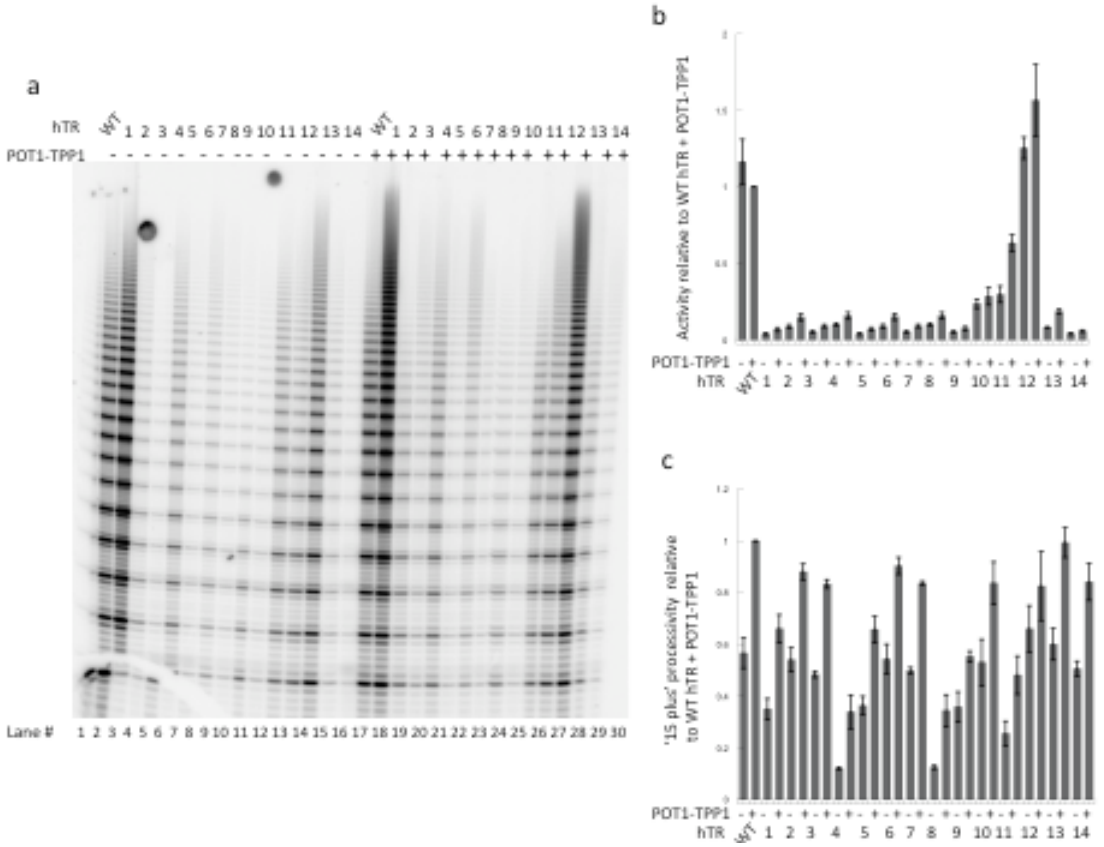

Figure 21 – Mutations made in the telomerase RNA pseudoknot region does not yield conclusive information on POT1-TPP1 interaction sites. (a) A direct telomerase extension assay using HEK 293T cell extracts and primer a5 at 1 μM. The extracts contain wild-type hTR or a mutated version of the RNA, each construct either in the presence or absence of POT1-TPP1. The first lane contains wild-type hTR in the absence of POT1-TPP1, and each subsequent lane contains hTR mutant number 1 thru 14. Lane 16 contains wild-type hTR in the presence of POT1-TPP1, and each subsequent lane contains hTR mutant number 1 thru 14. The number of telomeric hexad repeats is indicated on the left side. (b) Mean total activity of three independent experiments, normalized to the reaction with wild-type hTR and POT1-TPP1. Error bars show standard deviations. (c) Mean repeat addition processivity of three independent experiments, normalized to the reaction with wild-type hTR and POT1-TPP1. Error bars show standard deviations.

enough to lead to processivity stimulation. While a more extreme interpretation is that the protein complex does not interact with the pseudoknot/template domain, it is more likely that the small changes to hTR were not large enough to disrupt the TPP1-telomerase interaction interface. The mutation of a couple nucleotides in the telomerase RNA may not be a substantial enough

change in the enzyme to prevent the POT1-TPP1 heterodimer from interacting with the enzyme and providing its typical enhancement.

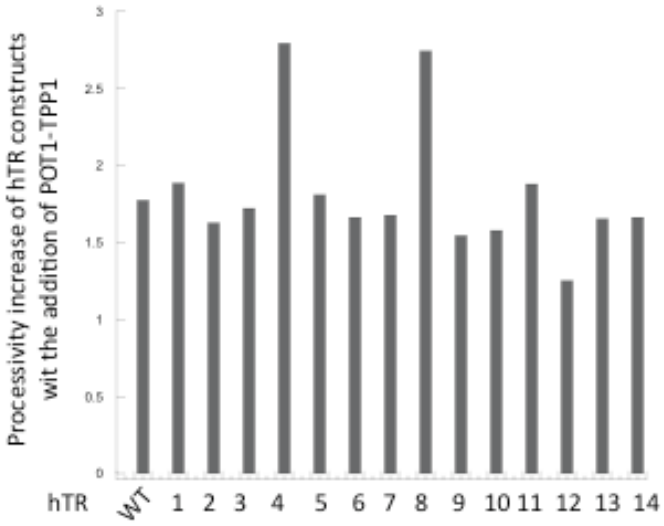

Figure 22 – The processivity increase for each human telomerase RNA construct with the addition of POT1-TPP1. From the same three independent experiments displayed in Figure 21, the height of the bars is representative of the number of times processivity increased with the addition of POT1-TPP1 (as averages from the three experiments). There is no normalization for this calculation. Wild-type processivity increased by about 1.5-fold, while mutants 9-12 notably only show a .5-fold enhancement of processivity.

4.3 – Materials and Methods

hTR site-directed mutagenesis: QuickChange® Site-Directed Mutagenesis Kit from Agilent Technologies was used. Fully complementary mutagenic primers were used to create 5-nucleotide mutations in the P1b helix of human telomerase RNA. The plasmids used were either pBS-U1 full-length or Δ1-32 as the template for PCR. 50 µl PCR reactions contained 1 µl pfu

polymerase, 5 µl pfu polymerase reaction buffer, 0.5 µl dNTP mix (25 mM each), 37.5 µl Elution Buffer (EB, QIAGEN), 3 µl DMSO (dimethyl sulfoxide), 1 µl each of top and bottom primers (15 µM), and 1 µl plasmid (100 ng/µl). The two primer sets used for P1b helix experiments changed nucleotides 33 thru 37 from 5'-GGCCA to 5'-CCGGU and nucleotides 187 thru 191 from 5'-UGGCC to 5'-ACCGG. Mutations made in hTR plasmids for disease-associated changes are referred to in the text. PCR cycle program was 1 minute at 95ºC, 50 seconds at 95ºC, 50 seconds at 60ºC, 5 minutes at 68ºC (repeat 95-60-68ºC cycle 18 times), 7 minutes at 68ºC, and 4ºC staying temperature. Dpn1 digests were done using 1 µl Dpn1 enzyme, and incubating reactions for 98 minutes at 37ºC. XL10-Gold Ultracompetent Cells were used for transformation and amplification of mutagenized plasmids (40 µl of cells, 4 µl of DNA). DNA was harvested from *E. coli* and purified according to QIAGEN® Miniprep procedures. Isolated plasmids were then sent to Davis Sequencing for confirmation of the desired sequence. Correctly mutagenized plasmids were then used to retransform XL10-Gold Ultracompetent Cells (40 µl of cells, 4 µl of DNA), which were subsequently grown in 500 ml cultures. DNA was harvested from the *E. coli* cultures and purified according to QIAGEN® Maxiprep procedures.

HEK 293T cell transfection and extract preparation: 2.5×10^6 cells per T25 flask were plated in 6 mls of media with antibiotics and incubated for 24 hours prior to transfection. Transfections used Lipofectamine 2000 (Invitrogen), 2.5 µg pVan 107, and 7.5 µg pBS-U1 (mutant or wild-type) in each transfected flask. Transfections yielding POT1 or TPP1 used 2.5 µg of p3X-Flag-POT1-Bl4 and 1 µg p3X-Flag-TPP1-Bl4. Control transfections (transfections without POT1 or TPP1) were performed using an empty pBl4 plasmid. Media without antibiotics was removed after 4-6 hours and replaced with fresh media containing Pen/Strep antibiotics. Cell lines incubated for 48 hours, were trypsinized, washed with PBS, resuspended in 500 µl CHAPS lysis

buffer (10 mM Tris-HCl pH 7.5, 1 mM $MgCl_2$, 1 mM EGTA, 0.5% CHAPS, 10% glycerol) and 3 µl RNasin plus (Promega). This mixture was nutated at 4ºC for 30 minutes, and then centrifuged for 10 minutes at 13,200 rpm. Supernatant was removed and added to a 75 µl FLAG bead slurry (1X human telomerase buffer, 30% glycerol), and then nutated at 4ºC overnight. The beads were then washed five times in 1x human telomerase buffer (30% glycerol), resuspended in 50 µl of the buffer, and flash frozen and stored at -80ºC.

Direct telomerase assay (*in vivo*): 20 µl telomerase reactions contain 50 mM Tris-Cl (pH 8.0), 30 mM KCl, 1 mM $MgCl_2$, 1 mM spermidine, 5 mM b-mercaptoethanol, 1 µM primer a5 or b, 500 µM dATP, 500 µM dTTP, 2.92 µM unlabelled dGTP, 0.33 µM radiolabelled dGTP (3000 Ci/mmol), and 6 µl of FLAG beads nutated with HEK293T cell lysate. Reactions are incubated at 30ºC for one hour. Reactions were stopped with 100 µl of 3.6 M ammonium acetate, 20 µg of glycogen. Products were precipitated with ethanol, then washed. Pellets were resuspended in 10 µl H20 and 10 µl loading buffer (95% formamide, 5% H20, loading dye). Samples were heated for 5 minutes at 95ºC for 5 minutes, centrifuged at 13,200 rpm for 10 minutes, and loaded onto a 10% acrylamide (7M urea, 1X TBE) sequencing gel. Gels were run for 1.75 hours at 90 Watts, dried, exposed to an image plate, and imaged on a phosphorimager (GE). Data was finally analyzed using Imagequant TL software.

Total activity quantification: Gels were quantitated using the Imagequant TL computer program. Total activity was obtained by getting the total number of counts in each individual lane (not including the loading control), using the 'rolling ball' background correction option in the program (usually at ~200). These numbers were normalized to the counts in the corresponding lane's loading control. For data representation, each lane was then normalized to the total activity of the 'standard' or 'wild-type' lane, which would numerically be considered '1.' Each

lane's numerical activity then is representative of its percentage of activity relative to the standard reaction (36).

Repeat addition processivity quantification, '15 plus': This was the preferred processivity quantification methodology because of the high repeat number bands generated when using cell lysate overexpressing telomerase. Instead of getting the signal in each individual band of the ladder, just one basic ratio was taken – the total counts of the lane 15 repeats and above divided by the total activity of the entire lane. More processive reactions generate larger ratios, while less processive reactions generate smaller ratios. Data representation, similar to the other methodologies, normalized the ratios to the ratio of the 'standard' or 'wild-type' lane, which would numerically be considered 'l.' Each lane's processivity value is then representative of its percentage of processivity relative to the standard reaction.

Section 5 – Discussion

The ways in which POT1 and TPP1 protect the telomeres from damage, shortening, and non-homologous end joining is relatively well documented. TPP1 is recruited to the telomere through interactions with TIN2, and POT1 is then recruited to the telomere through interactions with TPP1 (31, 32). The N-terminal OB domains of the POT1 protein can bind GGTTAG repeats of single stranded DNA at the 3' end overhang of the telomere (47). The repeated binding of TPP1 and then POT1 at the chromosome termini (54) serve to coat the 3' end completely, distinguishing it from a DNA break and preventing DNA repair processes.

The mechanisms by which POT1 and TPP1 interact with telomerase for enhancement at the telomere, however, are less well defined. TPP1 increases telomerase activity and processivity *in vitro*, though it seems to require POT1 presence for processivity stimulation and not activity stimulation (33, 36). TPP1 *in vivo* can also associate with telomerase at the telomere independently of POT1 (30). Recruitment and association of telomerase appears to require the TPP1-OB domain, implicating the OB fold in participating in an interaction with telomerase (30, 33). The main goal of this work was to identify the telomerase-associated surface of TPP1-OB using a site-directed mutagenesis strategy to reveal residues that cause functional defect in telomerase association and processivity.

Mutated surface sites on the TPP1-OB domain were selected because of high evolutionary conservation among mammals (**Figure 11a** and **b**). Fourteen TPP1-OB mutants were then expressed recombinantly in bacteria and tested to see if the single or double mutations appeared to alter structural integrity or binding of TPP1-POT1 (**Figure 11c**). Since mutations were small and on the surface, and the OB domain is not involved in POT1 binding interactions, it was anticipated that the mutations would not interfere with TPP1's enhancement of POT1-

DNA binding. As expected, an electrophoretic mobility shift assay demonstrated the ability of TPP1-OB mutants to bind POT1-DNA like wild-type (**Figure 12a**). Likewise, filter binding assays demonstrated that the TPP1-OB mutants enhanced POT1-DNA binding affinity in a wild-type-like manner (**Figure 12b**). These experiments verified that the mutations introduced on the TPP1-OB domain surface did not disturb the integrity of the protein or interfere with its typical POT1 related functions.

After this verification, mutants were used in direct telomerase extension assays to examine the mutations' effects on telomerase activity and processivity *in vitro*. These assays primarily used primer a5 since it forces POT1-TPP1 to bind at the 5' end, leaving the 3' end open for telomerase access and extension of the primer. Mutants L104A, D166A/E168A, E169A/E171A, E178A, R180A, L183A, R208V, and L212A substantially reduced the ability of the POT1-TPP1-N complex to stimulate activity (**Figure 13a** and **b**) and processivity (**Figure 13a** and **c**; **Figure 17a**) when compared to wild-type TPP1-N. Since the ability of POT1-TPP1 to stimulate telomerase activity is due to TPP1 alone, assays were also performed with all of the mutants in the absence of POT1. This result implicated the same group of mutants in a functional defect regarding telomerase activity stimulation (**Figure 14a**, **b**, and **c**). Direct telomerase extension assays were then performed using primer b to see if results were dependent on primer use. Primer b, unlike primer a5, is purely telomeric in sequence and requires telomerase to compete with POT1-TPP1 for binding of the 3' end. The same cohort of eight functionally defective TPP1 mutants was identified, with the addition of E215A (**Figure 15a**, **b**, and **c**), thus the effects seen are primer-independent.

Since the human TPP1-N had been recombinantly expressed in bacteria, and the human POT1 in insect cells, a new approach was taken to ensure data collected was not due to artifacts

of the expression system. Mutated TPP1 proteins were co-expressed in HeLa cell lines with telomerase and POT1, then the lysates were used in direct telomerase extension assays. Activity and processivity stimulation defects were seen with mutants L104A, D166A/E168A, E169A/E171A, E178A, R180A, L183A, R208V, L212A, and E215A (**Figure 16b**, **c**, and **d**; **Figure 17b**). The resulting consistencies between the systems of expression confirmed that defects in enhancement of telomerase activity and processivity are not due to TPP1 expression outside of human cell lines. E215A was the only mutant in which a quantitative difference between the systems was found.

E215A exhibited wild-type-like stimulation of telomerase activity and processivity in assays using bacterially expressed TPP1 and primer a5 (**Figure 13**), while showing moderate defects when used with primer b (**Figure 15**) or when co-expressed in HeLa cells (**Figure 16**). One possible explanation is difference in concentration between assays using bacterially expressed TPP1 and human cell expressed TPP1; the former uses a 500 nM concentration, while the latter has a more limiting amount of protein. The abundance of TPP1 has the potential to mask deleterious effects of the mutation, especially in the presence of such an easily extended primer (primer a5). It is also possible that E215 is a residue on the 'borderline' of the TPP1-telomerase interaction surface, thus exhibiting a moderate defect corresponding to its moderate involvement in the interaction.

While direct telomerase assays using TPP1-OB domain mutants revealed particular residues that reduce telomerase processivity stimulation, the data does not reveal much in terms of the nature of the telomerase-TPP1 interaction. The lowering of telomerase processivity could be due to decreased binding of telomerase to TPP1, or it could be due to a direct effect on a catalytic step of the telomerase reaction cycle. To help elucidate the nature of this interaction,

one of the lab members (Dr. Nandakumar) developed a co-immunoprecipitation assay (unpublished lab data). 3X-Flag TPP1, 3X-Flag POT1, and untagged telomerase (TERT and TR) were co-transfected, and lysate was nutated with anti-Flag beads. The anti-Flag beads do not pull down TERT in the absence of TPP1, but will pull down TERT in the presence of TPP1. The quantity of TERT pulled down is even further enhanced in the presence of POT1 and TPP1, maybe due to the stabilization by heterodimer formation. Each mutant was individually co-transfected, and the same pull down analysis was performed to see if certain mutants appeared defective in their abilities to pull down TERT. This served to examine whether or not the defects in the direct telomerase extension assays were due to a disruption of the TPP1-telomerase interface. Indeed, mutants D166A/E168A, E169A/E171A, E178A, R180A, L183A, R208V, L212A, and E215A, all showed a defect in binding and pulling down TERT efficiently. The only previously implicated mutant that did not exhibit this defect was L104A. All other mutants, like in the direct telomerase extension assays, behaved like wild-type. It is possible that L104A represents a residue that is important for stimulating telomerase processivity, while not being involved in the process of telomerase association, but this seems unlikely. It is more likely that L104A in the direct telomerase extension assay conditions was unstable, but was stable in the co-immunoprecipitation conditions.

The results of the co-immunoprecipitation and the primer extension assays together suggest that TPP1 is a binding factor that helps to regulate telomerase processivity in the context of TPP1-POT1-DNA. This aligns with previous research demonstrating that POT1-TPP1 decreases the off-rate of telomerase during its catalytic cycle and promote translocation (49); each of these elements helps increase the processivity of the enzyme. A mutagenesis approach to the project allowed for exploration of highly conserved amino acid residues on the surface of

TPP1's OB fold, elucidating the face of the protein that mediates the telomerase interaction. E168, E169, E171, E178, R180, L183, R208, L212, and E215 are the nine amino acids that are important for both telomerase processivity enhancement and association. All of these residues, when mapped on to the TPP1-OB structure, are on one face of the protein (**Figure 23**, **orange residues**), which is proposed to be the primary telomerase binding face of TPP1. The mutated amino acids that continually behaved like wild-type protein cluster primarily on the opposing face of the protein domain (**Figure 23**, **aqua residues**), and are not important for telomerase association or processivity enhancement.

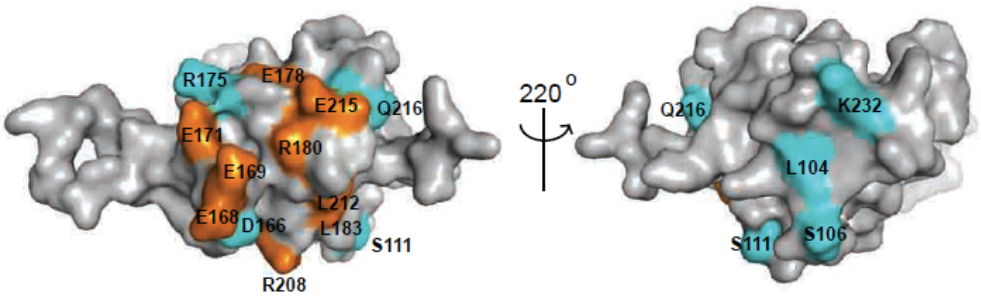

Figure 23 – TPP1 OB domain surface that determines telomerase association and enhancement. Two views of the surface of the TPP1 OB domain (structure solved in (36)). The implicated amino acid residues are colored in orange, and the wild-type-like mutants are colored in aqua. The left view, with a clustering of orange residues, shows the telomerase interaction

The implicated mutations made in the TPP1-OB domain can be deemed separation-of-function mutants. They do not impact TPP1's binding and enhancement of POT1, but do interfere with telomerase association functions. Without interfering in chromosome end protection functions, these mutations impact telomerase association and stimulation. This separation-of-function could be useful in the future to study the effects of poor telomerase stimulation without disrupting end protection machinery. Previous studies have relied upon total TPP1 knockdown as a means of elucidating TPP1 function (obliterating all of TPP1's typical

functions), so these findings could assist in a more nuanced approach. The project's results also further underscore the importance of POT1 in TPP1-mediated enhancement of telomerase. While it has been shown that TPP1 stimulates POT1's affinity for DNA, POT1 (in the co-immunoprecipitation assay) at the same time enhances TPP1's capacity to associate with telomerase. This highlights POT1 and TPP1 functioning as cooperative heterodimer, each individual protein complementing and optimizing the function of the other.

Yet studies on telomerase recruitment using telomere-ChIP of TERT and localization of telomerase at the telomere find that POT1 is dispensable for TPP1-mediated telomerase recruitment. Instead, TIN2 is required for TPP1-mediated telomerase recruitment to the telomere (30). A recent study on TIN2 mutations in dyskeratosis congenita (a telomerase dysfunction-based disease) demonstrated that a region on the TIN2 protein that is not involved in TPP1 binding is important for telomerase recruitment (55). This raises the possibility of yet another association site for telomerase at the telomere. Considering this information and the data of this project together, it seems that low levels of TIN2 and TPP1 would be sufficient to recruit telomerase to the telomere in the absence of POT1. After recruitment POT1 then is a necessary component for telomerase processivity and telomere extension. This reconciliatory hypothesis would need to be specifically tested. In this project, however, the absence of stoichiometric amounts of TIN2 in the direct telomerase extension assays makes POT1 and TPP1 necessary components for telomerase association with the telomere and subsequent extension.

Looking at the interaction of POT1 and TPP1 with telomerase at the telomere led to the examination of TPP1-telomerase surface contacts from the complementary perspective of the telomerase RNA. While mutation of the Gly100 residue of TERT had demonstrated an inability to be processively stimulated by POT1-TPP1, there have not been other TERT mutations with

such an effect. Additionally, the co-immunoprecipitation of TPP1 and telomerase appears to be dependent on the presence of telomerase RNA (unpublished lab data), so a similar mutagenesis strategy with the RNA was attempted in an effort of elucidate the nature of the TPP1-telomerase interaction.

It has been indicated that it is the pseudoknot/template domain interacting with the POT1-TPP1 heterodimer. Mixing and matching of mouse and human telomerase and POT1-TPP1 components revealed that human POT1-TPP1 requires a human pseudoknot/template domain to stimulate telomerase activity and processivity; the human complex did not require human TERT to cause stimulation (50). Preliminary lab data had also shown that humanization of the mouse pseudoknot domain via addition of a P1 helix led to activity and processivity enhancement with the addition of human POT1-TPP1, indicating a potential interaction site. When this hypothesis was investigated further, however, the potential identification of an interaction site appeared to be too forward of a conjecture. Using telomerase with a perturbed P1b helix on the RNA component did not eliminate POT1-TPP1's activity or processivity enhancement (**Figure 19**), as would have been expected if P1b was the interaction site for the heterodimer. One potential explanation for the enhancement seen with the humanization of mouse telomerase RNA is the increased stability imparted by P1 helix addition. Along with the enhanced stability is the potential lowering of free energy required to clear certain rate-limiting catalytic steps like translocation. The humanized mouse enzyme would have been able to move through processive telomerase actions with greater ease.

Section 6 - References

1. Greider, C.W. & Blackburn, E.H. A telomeric sequence in the RNA of *Tetrahymena* telomerase required for telomere repeat synthesis. *Nature* **337**, 331-337 (1989).

2. Lingner, J. et al. Reverse transcriptase motifs in the catalytic subunit of telomerase. *Science* **276**, 561-567 (1997).

3. Kelleher, C., Teixeira, M. T., Forstemann, K. & Lingner, J. Telomerase: biochemical considerations for enzyme and substrate. *Trends Biochem. Sci.* **27**, 572-579 (2002).

4. Autexier, C. & Lue, N.F. The structure and function of telomerase reverse transcriptase. *Annu. Rev. Biochem.* **75**, 493-517 (2006).

5. Yu, G., Bradley, J. D., Attardi, L.D. & Blackburn, E. H. *In vivo* alteration of telomere sequences and senescence caused by mutated *Tetrahymena* telomerase RNAs. *Nature* **344**, 126-132 (1990).

6. Yu, G. & Blackburn, E. H. Developmentally programmed healing of chromosomes by telomerase in *Tetrahymena*. *Cell* **67**, 823-832 (1991).

7. Qiao, F., Cech, T. R. Triple-helix structure in telomerase RNA contributes to catalysis. *Nat Struct Mol Biol* **15**, 634-640 (2008).

8. Chen, J. L., Blasco, M. A., Greider, C. W. Secondary structure of vertebrate telomerase RNA. *Cell* **100**, 503-14 (2000).

9. Romero, D. P., Blackburn, E. H. A conserved secondary structure for telomerase RNA. *Cell* **67**, 343-353 (1991).

10. Collins, K. & Mitchell, J. R. Telomerase in the human organism. *Oncogene* **21**, 564-579 (2002).

11. Feng, J. et al. The RNA component of human telomerase. *Science* **269**, 1236-1241 (1995).

12. Fu, D. & Collins, K. Human telomerase and Cajal body ribonucleoproteins share a unique specificity of Sm protein association. *Genes Dev.* **20**, 531-536 (2006).

13. Mitchell, J. R. & Collins, K. Human telomerase activation requires two independent interactions between telomerase RNA and telomerase reverse transcriptase *in vivo* and *in vitro*. *Mol. Cell* **6**, 361-371 (2000).

14. Pogacic, V., Dragon, F. & Filipowicz, W. Human H/ACA small nucleolar RNPs and telomerase share evolutionarily conserved proteins NHP2 and NOP10. *Mol. Cell. Biol.* **20**, 9028-9040 (2000).

15. Dragon, F., Pogcic, v. & Filipowicz, W. *In vitro* assembly of human H/ACA small nucleolar RNPs reveals unique features of U17 and telomerase RNAs. *Mol. Cell. Biol.* **20**, 3037-3048 (2000).

16. Tomlinson, R. L., Ziegler, T. D., Supakorndej, T., Terns, R. M. & Terns, M. P. Cell cycle-regulated trafficking of human telomerase to telomeres. *Mol. Biol. Cell* **17**, 955-965 (2006).

17. Zhu, Y., Tomlinson, R. L., Lukowiak, A. A., Terns, R. M. & Terns, M. P. Telomerase RNA accumulates in Cajal bodies in human cancer cells. *Mol. Biol. Cell* **15**, 81-90 (2004).

18. Collins, K. Physiological assembly and activity of human tellmerase complexes. *Mech. Ageing Dev.* **129**, 91-98 (2008).

19. Venteicher, A. S., et al. A human telomerase holoenzyme protein required for Cajal body localization and telomere synthesis. *Science* **323**, 644-648 (2009).

20. de Lange, T., Lundblad, V., Blackburn, E. Telomeres, Second Edition. *Cold Spring Harbor Laboratory Press*: New York (2006).

21. de Lange, T. Shelterin: the protein complex that shapes and safeguards human telomeres. *Genes Dev.* **19**, 2100-2110 (2005).

22. Liu, D., O'Connor, M. S., Qin, J., Songyang, Z. Telosome, a mammalian telomere-associated complex formed by multiple telomeric proteins. *J. Biol. Chem.* **279**, 51338-51342 (2004).

23. Broccoli, D., Smogorzewska, A., Chong, L., de Lange, T. Human telomeres contain two distinct Myb-related proteins, TRF1 and TRF2. *Nat. Genet.* **17**, 231-235 (1997).

24. Stansel, R. M., de Lange, T., Griffith, J. D. T-loop assembly in vitro involves binding of TRF2 near the 3' telomeric overhang. *EMBO J.* **20**, 5532-5540 (2001).

25. Chen, Y., Yang, Y., van Overbeek, M., Donigian, J. R., Baciu, P., et al. A shared docking motif in TRF1 and TRF2 used for differential recruitment of telomeric proteins. *Science* **319**, 1092-1096 (2008).

26. Li, B., de Lange, T. Rap1 affects the length and heterogeneity of human telomeres. *Mol. Biol. Cell* **14**, 5060-5068 (2003).

27. Li, B., Oestreich, S., de Lange, T. Identification of human Rap1: implications for telomere evolution. *Cell* **101**, 471-483 (2000).

28. Ye, J. Z., Donigian, J. R., van Overbeek, M., Loayza, D., Luo, Y., et al. TIN2 binds TRF1 and TRF2 simultaneously and stabilizes the TRF2 complex on telomeres. *J. Biol. Chem.* **279**, 47264-47271 (2004).

29. O'Connor M. S., Safari, A., Xin, H., Liu, D., Songyang, Z. A critical role for TPP1 and TIN2 interaction in high-order telomeric complex assembly. *Proc. Natl. Acad. Sci. USA* **103**, 11874-11879 (2006).

30. Abreu, E., et al. TIN2-tethered TPP1 recruits human telomerase to telomeres *in vivo*. *Mol. Cell. Biol.* **30**, 2971-2982 (2010).

31. Liu, D., Safari, A., O'Connor, M. S., Chan, D. W., Laegeler, A., et al. PTOP interacts with POT1 and regulates its localization to telomeres. *Nat. Cell Biol.* **6**, 673-680 (2004).

32. Ye, J. Z., Hockemeyer, D., Krutchinsky, A. N., Loayza, D., Hooper, S. M., et al. POT1-interacting protein PIP1: a telomere length regulator that recruits POT1 to the TIN2/TRF1 complex. *Genes Dev.* **18**, 1649-1654 (2004).

33. Xin, H., Liu, D., Wan, M., Safari, A., Kim, H., et al. TPP1 is a homologue of ciliate TEBP-beta and interacts with POT1 to recruit telomerase. *Nature* **445**, 559-562 (2007).

34. Hockemeyer, D., Palm, W., Else, T., Daniels, J. P., Takai, K. K., et al. Telomere protection by mammalian POT1 requires interaction with TPP1. *Nat. Struct. Mol. Biol.* **14**, 754-761 (2007).

35. Baumann, P., Cech, T. R. POT1, the putative telomere end-binding protein in fission yeast and humans. *Science* **292**, 1171-1175 (2001).

36. Wang, F., Podell, E. R., Zaug, A. J., Yang, Y., Baciu, P., et al. The POT1-TPP1 telomere complex is a telomerase processivity factor. *Nature* **445**, 506-510 (2007).

37. de Lange, T. et al. Structure and variability of human chromosome ends. *Mol. Cell Biol.* **10**, 518-527 (1990).

38. Kipling, D. & Cooke, H. J. Hypervariable ultralong telomeres in mice. *Nature* **347**, 400-402 (1990).

39. Palm, W. & de Lange, T. How Shelterin Protects Mammalian Telomeres. *Ann. Rev. of Gen.* **42**, 301-334 (2008).

40. McElligott, R. & Wellinger, R. J. The terminal DNA structure of mammalian chromosomes. *EMBO J.* **16**, 3705-3714 (1997).

41. Hockemeyer, D., Sfeir, A. J., Shay, J. W., Wright, W. E., de Lange, T. POT1 protects telomeres from a transient DNA damage response and determines how human chromosomes end. *EMBO J.* **24**, 2667-2678 (2005).

42. Griffith, J.D. et al. Mammalian telomeres end in a large duplex loop. *Cell* **97**, 503-514 (1999).

43. Shiloh, Y. ATM and related protein kinases: safeguarding genome integrity. *Nat. Rev. Cancer* **3**, 155-168 (2003).

44. Olovnikov, A. M. A theory of marginotomy. The incomplete copying of template margin in enzymic synthesis of polynucleotides and biological significance of the phenomenon. *J. Theor. Biol.* **41**, 181-190 (1973).

45. Smogorzewska, A., de Lange, T. Regulation of telomerase by telomeric proteins. *Annu. Rev. Biochem.* **73**, 177-208 (2004).

46. van Steensel, B. de Lange, T. Control of telomere length by the human telomeric protein TRF1. *Nature* **385**, 740-743 (1997).

47. Lei, M., Podell, E. R., Cech, T. R. Structure of human POT1 bound to telomeric single-stranded DNA provides a model for chromosome end-protection. *Nat. Struct. Mol. Biol.* **11**, 1223-1229 (2004).

48. Denchi, E. L., & de Lange, T. Protection of telomeres through independent control of ATM and ATR by TRF2 and POT1. *Nature* **448**, 1068-1071 (2007).

49. Latrick, C. M. & Cech, T. R. POT1-TPP1 enhances telomerase processivity by slowing primer dissociation and aiding translocation. *EMBO J.* **29**, 924-933 (2010).

50. Zaug, A. J., Podell, E. R., Nandakumar, J., Cech, T. R. Functional interaction between telomere protein TPP1 and telomerase. *Genes Dev.* **24**, 613-622 (2010).

51. Chen, J. L., Blasco, M. A., Greider, C. W. Secondary structure of vertebrate telomerase RNA. *Cell* **100**, 503-514 (2000).

52. Collins, K. The biogenesis and regulation of telomerase holoenzymes. *Nat. Rev. Mol. Cell Bio.* **7**, 484-494 (2006).

53. Zaug, A. J., Podell, E. R., Cech, T. R. Mutation in TERT separates processivity from anchor-site function. *Nat Struct Mol Biol* **15**, 870-872 (2008).

54. Taylor, D.J., Podell, E.R., Taatjes, D.J., Cech, T.R. Multiple POT1-TPP1 proteins coat and compact long telomeric single-stranded DNA. *J Mol Biol* **410**, 10-17 (2011).

55. Calado, R. T., Young, N. S. Telomere maintenance and human bone marrow failure. *Blood* **111**, 4446-4455 (2008).

56. Feng, J., Funk, W. D., Wang, S. S., Weinrich, S. L., Avilion, A. A., Chiu, C. P., Adams, R. R., Chang, E., Allsopp, R. C., Yu, J. et al. The RNA component of human telomerase. *Science* **269**, 1236-1241 (1995).

57. Marrone, A., Sokhal, P., Waine, A., Beswick, R., et al. Functional characterization of novel telomerase RNA (TERC) mutations in patients with diverse clinical and pathological presentations. *Haematologica* **92**, 1013-1020 (2007).

58. Vulliamy, T. J., Marrone, A., Knight, S. W., Walne, A., Mason, P. J., Dokal, I. Mutations in dyskeratosis congenita: their impact on telomere length and the diversity of clinical presentation. *Blood* **107**, 2680-2685 (2006).

59. Armanios, M. Y., Chen, J. J., Cogan, J. D., Alder, J. K., et al. Telomerase mutations in families with idiopathic pulmonary fibrosis. *N Engl J Med* **356**, 1317-1326 (2007).

60. Ortmann, C. A., Neimeyer, C. M., Wawer, A., Ebell, W., Baumann, I., Kratz, C. P. TERC mutations in children with refractory cytopenia. *Haematologica* **91**, 707-708 (2006).